Economic Geology
Vol. 98, 2003, pp. 69–86

Compositional Variations of Olivine and Sulfur Isotopes in the Noril'sk and Talnakh Intrusions, Siberia: Implications for Ore-Forming Processes in Dynamic Magma Conduits

Chusi Li,† Edward M. Ripley,

Department of Geological Sciences, Indiana University, Bloomington, Indiana 47401

and Anthony J. Naldrett

Department of Geology, University of Toronto, Toronto, Ontario, Canada M5S 3B1

Abstract

Olivine from the Noril'sk I, Main and Northwestern Talnakh ore-bearing intrusions in the Noril'sk region occurs as inclusions, discrete grains, and poikilitic crystals. The original compositions of olivine inclusions have been well preserved by their host oikocrysts from reaction with interstitial silicate and sulfide liquids. In contrast, the compositions of discrete and poikilitic olivine crystals have been variably modified by reequilibration with trapped silicate and sulfide liquids. There are abrupt changes in the contents of nickel in olivine inclusions (500–1,500 ppm) between different rock units in all three intrusions, which indicates that the different rock units in these intrusions are not related to each other via in situ differentiation of a common parental magma but rather are consistent with separate pulses of magma with variable degrees of differentiation, possibly involving olivine crystallization and assimilation of siliceous crustal material in a staging chamber.

The $\delta^{34}S$ values of the samples with high sulfur contents (>800 ppm sulfur) from all three ore-bearing intrusions vary between 8 and 14 per mil. Two sulfur-poor samples (<600 ppm sulfur) from the Northwestern Talnakh intrusion yield $\delta^{34}S$ values of 1.5 and 3.6 per mil. These values are similar to the values of the sulfur-poor rocks from the ore-barren intrusions in the region and illustrate the fact that high sulfur contents couple with increasing $\delta^{34}S$ values. Such a relationship is consistent with the addition of crustally derived ^{34}S-enriched sulfur to the magma of the ore-bearing intrusions.

In contrast to other models of sulfide segregation in closed systems, we propose that sulfide segregation occurred in an open system and the magma involved was undersaturated in sulfur and undepleted in chalcophile elements. We envision that the ^{34}S-enriched sulfur was introduced via circulating fluids that transported sulfur from evaporite in the underlying sedimentary sequence to the magma in a dynamic magma conduit. The immiscible sulfide liquids that segregated during sulfur contamination settled down in the wider parts of the conduit as the magma continued to travel. Successive pulses of new magma entered the conduit, reacted with the early sulfide, and displaced much of the early magma in the conduit. The ore-bearing intrusions are thought to have crystallized within the wider parts of the conduits and their voluminous, sulfide-poor peripheral sills represent some (if not all) of the magma that flowed out of the conduits.

Introduction

The Ni-Cu-PGE (platinum-group elements) ore-bearing intrusions of the Noril'sk-Talnakh area have been shown by U-Pb dating (Kamo et al., 1996, 2000) to be contemporaneous with the voluminous Permo-Triassic Siberian traps flood basalts. The most important ore-bearing intrusions in the area are the Noril'sk I, Main and Northwestern Talnakh intrusions. Czamanske et al. (1994, 1995) and Zen'ko and Czamanske (1994a, b) referred to the Northwestern Talnakh intrusion as the Kharaelakh intrusion and the Main Talnakh intrusion as the Talnakh intrusion. Many researchers suggested that the intrusions are sills formed by the emplacement of sulfide-bearing magmas derived from a dynamic staging magma chamber (Naldrett et al., 1992; Brügmann et al., 1993; Naldrett and Lightfoot, 1993; Fedorenko, 1994; Lightfoot et al., 1994) or a series of staging magma chambers (Distler et al., 1986). Czamanske et al. (1995) also favored a model involving sulfide magma emplacement. Naldrett et al. (1995, 1996), Lightfoot and Hawkesworth (1997), and Naldrett and Lightfoot (1999) proposed that the ore-bearing intrusions were subvolcanic feeders in which immiscible sulfide liquids carried by the ascending magmas accumulated and subsequently reacted with continuous surges of new magma enroute to the surface to form lavas. These authors suggested that initial sulfide saturation resulted from contamination by siliceous crustal material in a staging chamber. Based on the results of phase equilibria studies, Latypov (2002) concluded that the parental magmas of the ore-bearing intrusions and associated lavas cannot be related through fractional crystallization and the association of chalcophile element-depleted lavas with the ore-bearing intrusions is coincidental. Sulfur isotope studies by Gorbachev and Grinenko (1973) and Grinenko (1985) showed that the sulfide ores are characterized by elevated $\delta^{34}S$ values ranging from 6 to 16 per mil. Evaporites found within the sedimentary country rocks are characterized by $\delta^{34}S$ of about 20 per mil (Gorbachev and Grinenko, 1973) and provide an ample reservoir of ^{34}S-enriched sulfur but sour gas accumulations could have been an alternative source of sulfur. Studies of the sulfide ores by Naldrett et al. (1992, 1996) and Zientek et al. (1994) indicated that the combined concentrations of Pt + Pd may reach 100 ppm. Naldrett et al. (1992, 1996) emphasized that such high concentrations in an

† Corresponding author: e-mail, cli@indiana.edu

immiscible sulfide liquid that separated from a silicate magma with Pt and Pd concentrations of less than 20 ppb (similar to the values of chalcophile element-undepleted lavas in the Noril'sk region; Brügmann et al., 1993) would have required that the sulfide reacted with a volume of magma about 50 × greater than the volume of magma represented by the ore-bearing intrusions. In other words, the mass ratio of magma to sulfide liquid (R value of Campbell and Naldrett, 1979) would have been more than 2,000. In contrast, the volume of magma inferred from a simple isotopic mixing model of magma and evaporite ($\delta^{34}S$ = 20‰; Gorbachev and Grinenko, 1973) or sour gas ($\delta^{34}S$ = 10‰; Grinenko, 1985) would have been far less (more than one order of magnitude lower). These different models have not been resolved. Thus, the outstanding questions of sulfide ore formation at Noril'sk and Talnakh include the genetic relationship of different rock units in the ore-bearing intrusions, the genetic relationship of ore-bearing intrusions and associated lavas, the source and mechanism of sulfur contamination in the ore-bearing intrusions, and the origin of sulfide saturation. In this study we use olivine and sulfur isotope data to address these issues.

The Intrusions and Associated Lavas

Russian data, such as those present in Genkin et al. (1981) and Duzhikov et al. (1988) and those compiled during an earlier study by Naldrett et al. (1992), show that mineralization is associated with specific differentiated intrusions that are divided into two subgroups referred to as the Noril'sk and Lower Talnakh types (see Fedorenko et al., 1984; Fedorenko, 1994). These two groups are commonly spatially associated and occur close to the Noril'sk-Kharaelakh fault zone (Fig. 1). The Noril'sk-type intrusions are ore-bearing bodies and are best represented by the Noril'sk I, Main and Northwestern Talnakh intrusions. These three intrusions together contain much of the sulfide ore in the area (historic resource >555 Mt at 3.9 wt % Cu, 2.7 wt % Ni; Lightfoot and Hawkesworth, 1997). The Lower Talnakh-type intrusions include the Lower Noril'sk and Lower Talnakh intrusions and contain only subeconomic disseminated sulfide mineralization with low Ni, Cu, and PGE concentrations (Duzhikov et al., 1992). The Lower Talnakh intrusion occurs a few tens of meters directly below the Main and Northwestern Talnakh intrusions, whereas the Lower Noril'sk intrusion lies 5 to 10 km to the west of the Noril'sk I intrusion.

Figure 2 is a vertical section illustrating the spatial relationships between the Lower, Main, and Northwestern Talnakh intrusions. Naldrett et al. (1992) and Zen'ko and Czamanske (1994a) discuss evidence, which indicates that the Lower Talnakh-type intrusions were emplaced slightly before the Noril'sk type, although chilled zones are absent when these two types of intrusions are in direct contact.

Detailed descriptions of the ore-bearing intrusions have been given by Czamanske (2002). A brief description is given here. The ore-bearing intrusions are flat, elongated bodies (15 × 2 × 0.2 km) that intruded argillites, evaporates, and coal measures, as well as the lower part of a 3.5-km-thick volcanic sequence comprising an alternating series of lavas and tuffs. The overall structure of an ore-bearing intrusion is divisible into two distinct parts: a relatively restricted main body and peripheral sills (Zen'ko and Czamanske, 1994b; Czamanske et al., 1995). The peripheral sills are characterized by rather simple lithology and mainly consist of unmineralized olivine-bearing or olivine-free gabbro. In contrast, the main body is typically comprised of six rock units, in the ascending sequence of contact gabbro, taxitic (variably textured) gabbro, picritic gabbro, olivine gabbro, gabbro, and leucocratic gabbro. Duzhikov et al. (1992), Czamanske et al. (1994, 1995), and Zen'ko and Czamanske (1994a, b) have referred to the gabbroic rocks as gabbrodolerite in reflection of their subvolcanic textures. The thickness of rock units varies substantially from one intrusion to another and from one drill hole to another within the same intrusion (e.g., Zen'ko and Czamanske, 1994a). Zen'ko and Czamanske (1994b) report 0.2 wt percent sulfide in the Noril'sk I intrusion, 2.8 wt percent sulfide in the Main Talnakh intrusion, and 7.1 wt percent sulfide in the Northwestern Talnakh intrusion. The principal accumulations of sulfides (mainly pyrrhotite, pentlandite, and chalcopyrite) are of three types: (1) disseminated sulfides (2–10%) within picritic and taxitic gabbro units; (2) massive sheets, up to 3.5 × 1.5 × 0.05 km in size, at the base of and immediately underlying the intrusions; and (3) so-called copper ore (usually but not always chalcopyrite rich), forming a halo of disseminated sulfide in the sedimentary rocks enclosing massive ore or occupying breccia zones (Genkin et al., 1981; Duzhikov et al., 1988). The gabbroic rocks of the upper part of the intrusions are sulfide poor, but disseminated sulfide patches and

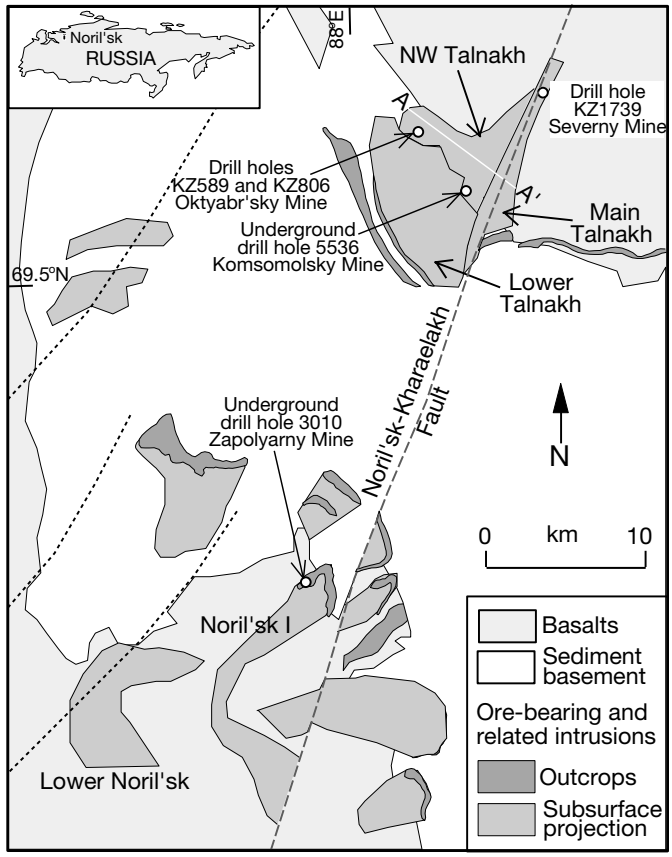

FIG. 1. Geologic plan showing the spatially close association of ore-bearing and related mafic intrusions in the Noril'sk-Talnakh area, Siberia (simplified from Naldrett and Lightfoot, 1999).

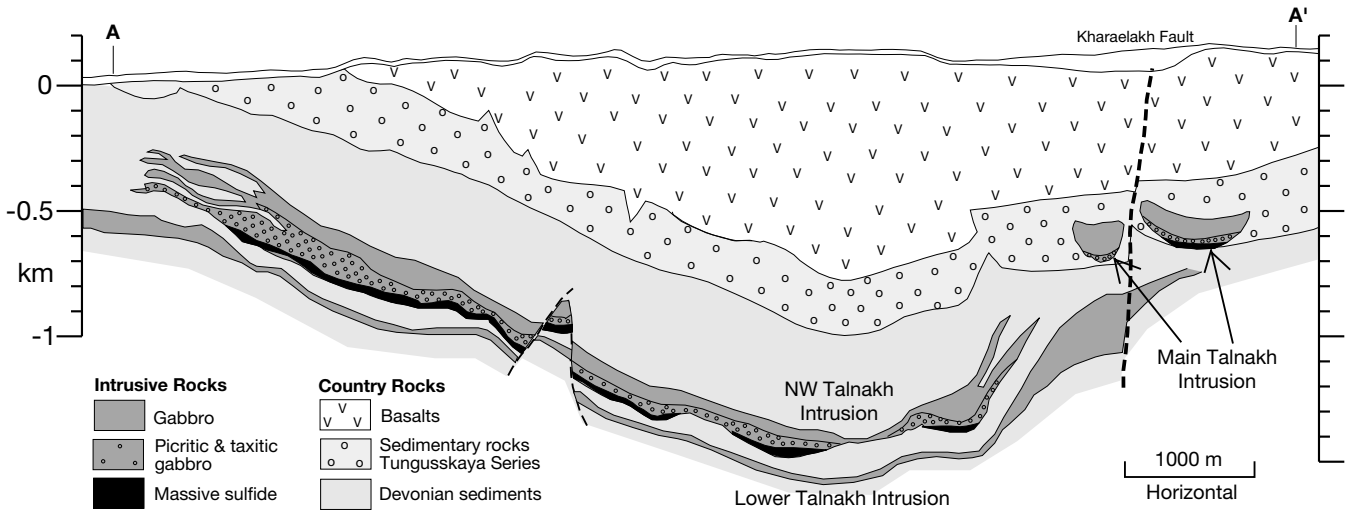

FIG. 2. Geologic cross section showing the relationship between the Main, Northwestern, and Lower Talnakh intrusions (simplified from Naldrett and Lightfoot, 1999).

small sulfide veins (a few centimeters wide) are often found in the lower olivine gabbro and contact gabbro underlying mineralized taxitic gabbro.

The complete basaltic sequence overlying the mineralized intrusions (Fig. 2) has been divided into 11 formations based on petrographic characteristics and chemical compositions (Fedorenko, 1981, 1994; Lightfoot et al., 1990, 1993; Wooden et al., 1993; Fedorenko et al., 1996; Lightfoot and Hawkesworth, 1997). The lavas that have been considered by these authors to be related to the intrusions are from the Tuklonsky (tk) to Morongovsky (mr_2) formations (see Table 1). Based on geologic, geochemical, and isotopic data, Fedorenko (1994) and Fedorenko et al. (1996) concluded that the Lower Talnakh- and Noril'sk-type intrusions were emplaced between the eruption of the Lower (mr_1) and Upper Morongovsky (mr_2) lavas. The studies of Naldrett et al. (1992) and Brügmann et al. (1993) indicate that the Lower and Middle Nadezhdinsky lavas (nd_{1-2}) have lost 75 percent of their Cu and Ni and more than 90 percent of their PGE compared to the underlying Tuklonsky lava (tk), the Upper Nadezhdinsky to Lower Morongovsky lavas (nd_3-mr_1) show a gradual increase in these chalcophile elements, and the overlying Upper Morongovsky and Mokulaevsky lavas (mr_2-mk) reach the values of the Tuklonsky lava (tk). The Lower and Middle Nadezhdinsky lavas (nd_{1-2}) are characterized by 5 to 15 percent contamination of granodioritic crustal materials, whereas other lavas record much less to undetectable crustal contamination (Lightfoot et al., 1990, 1993, 1994; Wooden et al., 1993; Fedorenko, 1994; Walker et al., 1994; Hawkesworth et al., 1995; Horan et al., 1995; Fedorenko et al., 1996).

TABLE 1. Summary of Seven Lower Suites of the Flood Basalts in the Noril'sk Area, Siberia

Lava suite		Whole-rock composition[1]					Predicted olivine composition		
(stratigraphic order)	Abbreviation	MgO (wt %)	FeO[2] (wt %)	Ni (ppm)	Cu (ppm)	Pd (ppb)	Fo[3]	Fo[4]	Ni[5] (ppm)
Mokulaevsky	mk	6.83	9.83	103	132	9		80.5	721
Upper Morongovsky	mr2	7.19	9.47	107	122	8		81.9	749
Lower Morongovsky	mr1	6.90	9.53	86	113	5		81.1	602
Upper Nadezhdinsky	nd3	6.57	8.77	81	97	<3		81.7	567
Middle Nadezhdinsky	nd2	6.07	8.55	45	87	<3		80.8	315
Lower Nadezhdinsky	nd1	6.32	7.81	23	32	<3		82.8	161
Tuklonsky	tk	8.99	8.40	110	101	12	85		770
Gudchichinsky	gd	6.57	8.62	83	71	<3		81.9	581
Syverminsky	sv	6.01	8.45	55	34	<3	80		385
Ivakinsky	iv	3.55	10.48	18	23			66.8	126

[1] Whole-rock MgO, FeO_{total}, Ni, and Cu concentrations are from Lightfoot et al. (1994); Pd contents are from Brügmann et al. (1993) and Fedorenko et al. (1996)

[2] FeO is adjusted from whole-rock FeO_{total} using MELTS of Ghiorso and Sack (1995) under QFM buffer and 1 bar P_{total}

[3] Olivine is predicted to be the first phase to crystalize from these lavas under 1 bar P_{total} according to MELTS (Ghiorso and Sack, 1995); Fo = mol % forsterite

[4] These lavas are not predicted to crystallize olivine under pressure up to mantle conditions according to MELTS; the compositions of olivine assumed to crystallize from these samples are calculated using the ratio of $(FeO/MgO)_{olivine}/(FeO/MgO)_{liquid}$ equal to 0.3 from Roeder and Emslie (1970)

[5] The content of Ni in olivine is calculated assuming the olivine/liquid partitioning coefficient equal to 7

Sampling and Analytical Methods

Olivine compositions and sulfur isotope data were obtained for 50 samples from three drill cores in three ore-bearing intrusions (Fig. 1): the Noril'sk I intrusion (hole 3010, drilled from an underground shaft), the Main Talnakh intrusion (hole KZ1739, drilled from surface), and the Northwestern Talnakh intrusion (hole 5536, drilled from an underground shaft). Additional samples were collected from other drill cores located in the Oktyabr'sky mine in the Northwestern Talnakh intrusion. The samples selected for this study are unmineralized or mineralized with disseminated sulfides up to 25 wt percent. Most of the samples are fresh, but local alteration such as replacement of plagioclase by a mixture of chlorite and epidote and replacement of pyroxene by amphibole and chlorite are found in some samples.

The compositions of olivine in all samples were determined by wavelength dispersive analysis using the CAMECA SX50 electron microprobe at Indiana University. An accelerating voltage of 15 kV was used. Beam current and counting time for major elements were 20 nA and 20 s, respectively. Nickel was analyzed at a beam current of 100 nA and a counting time of 100 s. The detection limit for Ni under these conditions was about 60 ppm. The accuracy of analyses was monitored using San Carlos olivine (USNM 1113122/444) reference material. Sample reproducibility varied by less than 2 percent. The tabulated olivine compositions are the averages of more than 10 analyses of the cores of olivine grains. The compositional variation from core to margin, as well as between different crystals is discussed below.

Disseminated sulfide minerals (pyrrhotite, pentlandite, and chalcopyrite) were drilled from the samples using a 0.75-mm carbide bit. Sulfide powders mixed with approximately 10 × V_2O_5 were loaded into tin capsules and analyzed using elemental analyzer-continuous flow isotope ratio mass spectrometry on a Finnigan MAT252 mass spectrometer. Analytical precision was better than ±0.05 per mil. Sample reproducibility was ±0.1 per mil. Sulfur isotope compositions are reported in standard δ notation relative to VCDT (Vienna Cañon Diablo Troilite).

Results for both olivine analyses and sulfur isotope ratios in coexisting sulfides are reported in Table 2.

Results

Types of olivine

Olivine from the Noril'sk I, Northwestern and Main Talnakh intrusions occurs as (1) inclusions in pyroxene and plagioclase oikocrysts (Fig. 3a-f), (2) discrete grains with granular or subpoikilitic pyroxene and plagioclase, and interstitial sulfides (Figs. 3f, 4a, b), and (3) poikilitic crystals enclosing pyroxene and plagioclase (Fig. 4c, d). Olivine inclusions are most common in the picritic gabbro unit, whereas poikilitic olivine is most common in the olivine gabbro unit. All three types of olivine have been observed in the taxitic gabbro unit.

Olivine inclusions are small (mostly <100 μm in diam) and rounded. In some samples, small chromite and sulfide inclusions (<20 μm in diam) coexist with olivine inclusions in a single oikocryst. Olivine inclusions are randomly oriented in most samples from the Noril'sk I and Main Talnakh intrusions (Fig. 3a, b) and are preferentially oriented in most samples from the Northwestern Talnakh intrusion, with laminated texture (Fig. 3e, f). Different generations of olivine characterized by different orientations and Fo contents (81 vs. ~77 mol %) are locally enclosed in a single oikocryst. In Figure 3e, the more primitive olivine inclusion (Fo ~81 mol %) is distinctly smaller.

Discrete olivine grains are generally larger than those that occur as inclusions, with grain size generally greater than 2 mm in diameter. They mostly exhibit subhedral to euhedral shapes. Poikilitic olivine crystals are much larger, varying between 5 and 10 mm in diameter. Small olivine inclusions always coexist with large discrete olivine grains in the same sample, resulting in a heterogeneous texture on the scale of the oikocryst dimensions. Domains of relatively large discrete olivine grains coexisting with granular pyroxene and plagioclase pass into domains with successively smaller olivine grains enclosed in poikilitic pyroxene or plagioclase (Fig. 3a, b). Smaller and more primitive olivine inclusions tend to occur toward the core of an oikocryst (Fig. 3c, d). Discrete olivine grains locally coexist with poikilitic olivine, but no poikilitic olivine has been found to coexist with olivine inclusions in the same sample.

A particular type of olivine occurs as irregular olivine-rich clots that have been referred to as "olivinite" by many Russian geologists (Duzhikov et al., 1992; Likhachev, 1994). Typical olivinite is characterized by granular to subpoikilitic textures and contains 70 to 90 modal percent small olivine grains (mostly <50 μm in diam), 10 to 30 percent interstitial and poikilitic phases, mostly clinopyroxene and plagioclase (Fig. 4e, f), and minor chromite inclusions in silicates and interstitial sulfides. Olivine in olivinite is always more primitive than that in the gabbroic to picritic host rocks. Olivinite is most common in the picritic gabbro unit, less common in the taxitic gabbro unit, and rare in the olivine gabbro unit. Its contact with the host rocks is commonly associated with plagioclase (Fig. 4e, f).

In cumulate terminology, olivine inclusions and poikilitic olivine may be described as cumulus and intercumulus phases, respectively. Discrete olivine crystals are either cumulus or intercumulus phases. Olivinite possibly represents xenolith of disrupted, early olivine cumulate.

Olivine compositional variations

The core to rim differences in forsterite (Fo) and Ni contents in olivine inclusions are small, mostly less than 0.8 mol percent and 120 ppm, respectively. The core to rim differences in discrete and poikilitic olivine crystals are slightly larger, up to 1.5 mol percent Fo and 300 ppm Ni, respectively. Representative compositional variations across single grains of large discrete and poikilitic olivine are shown in Figure 5. Nickel zonation is not evident but higher Fo contents (by 0.5–1.5 mol %) tend to occur toward the core of an olivine crystal.

The compositional relationship between different types of olivine in a single sample is illustrated in Figure 6a to h. Weak positive Ni-Fo correlation is apparent in olivine inclusions that are not associated with sulfide inclusions (Fig. 6b, e, and f). This relationship is not evident in olivine inclusions that are associated with sulfide inclusions (Fig. 6a, c, and d). The Fo contents in olivine inclusions and coexisting discrete

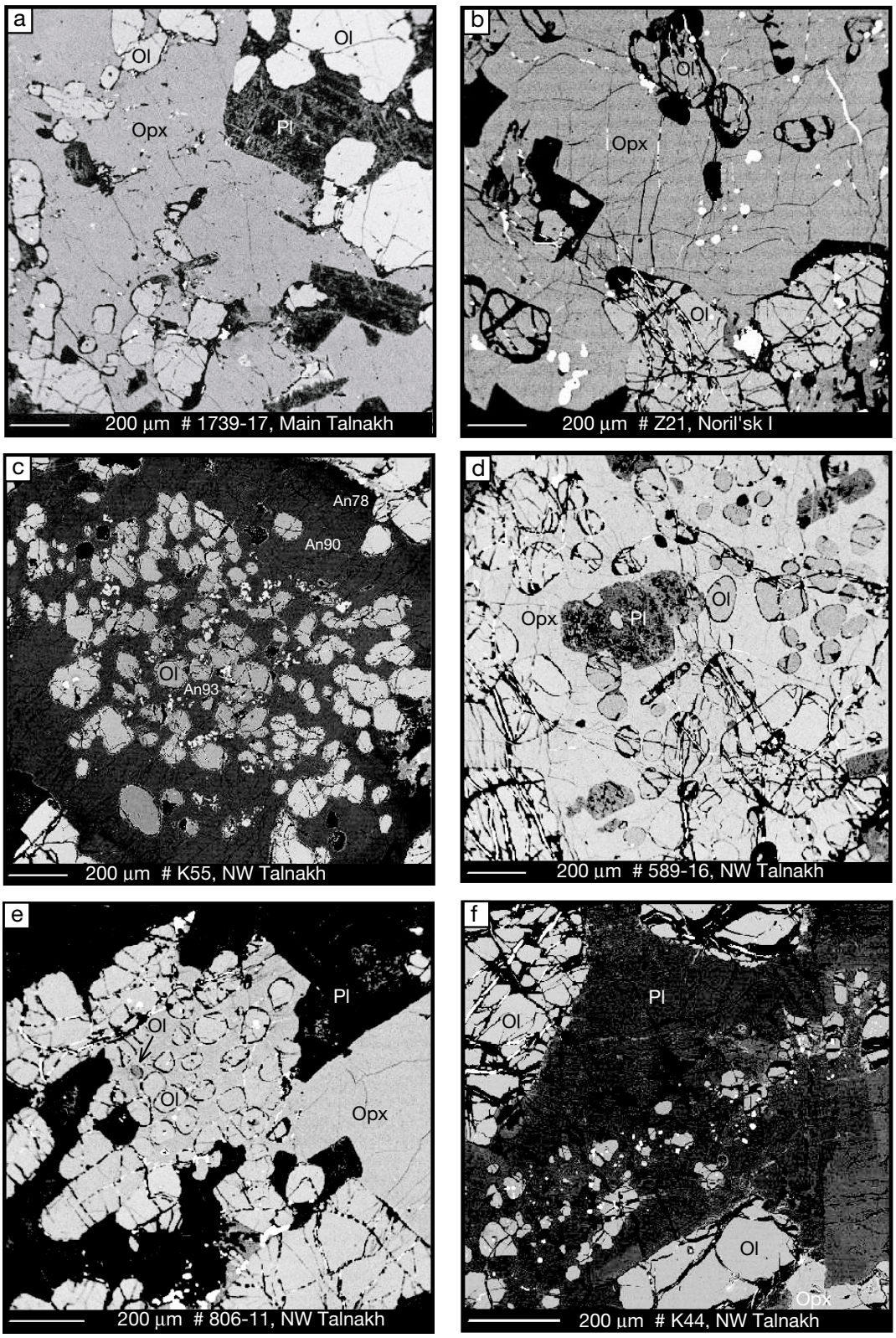

FIG. 3. Back-scattered electron (BSE) images showing representative textural relationships of olivine with other phases in picritic and taxitic gabbros. Olivine inclusions are smaller, contain higher Fo (forsterite, Mg_2SiO_4), and have darker BSE images than coexisting discrete grains (a) and (b). Smaller and more primitive (containing higher Fo) olivine inclusions tend to occur toward the core of a single host oikocryst (c) and (d). Preferentially oriented olivine inclusions occur in samples with lamination texture (e) and (f). An = anorthite (accompanied number is mole % An of plagioclase), Ol = olivine, Opx = orthopyroxene, Pl = plagioclase. Phases with the brightest BSE images are sulfide and spinel.

TABLE 2. Olivine and Isotope Compositions of Coexisting Sulfides

Sample no.	Depth or distance (m)	Type of olivine	Rock type	Olivine composition[1] (wt %) SiO_2	Cr_2O_3	MgO	CaO	MnO	FeO	NiO	Total	Forsterite (mol %)	Ni in Ol (ppm)	Sulfides $\delta^{34}S$	Whole rock S[2] (wt %)
Noril'sk I, drill core 3010, Zapolyarny mine[3]															
Z29	1	Inclusion	Picritic gabbro	39.38	0.027	41.90	0.12	0.26	17.41	0.265	99.37	80.99	2086		
Z29	1	Discrete crystal	Picritic gabbro	39.00	0.016	39.78	0.16	0.31	20.06	0.284	99.60	77.85	2230	9.6	0.82
Z28	1.6	Inclusion	Picritic gabbro	39.49	0.045	41.30	0.15	0.30	18.84	0.156	100.28	79.53	1222		
Z28	1.6	Discrete crystal	Picritic gabbro	39.39	0.049	40.22	0.20	0.30	20.29	0.162	100.61	77.90	1270	10.5	1.24
Z27	3.6	Inclusion	Picritic gabbro	39.21	0.023	40.79	0.11	0.32	19.38	0.233	100.07	78.80	1832		
Z27	3.6	Discrete crystal	Picritic gabbro	38.94	0.018	40.14	0.19	0.32	20.18	0.233	100.03	77.93	1828	10.0	0.34
Z26	5.3	Discrete crystal	Picritic gabbro	39.01	0.015	39.82	0.15	0.33	19.78	0.223	99.34	78.09	1752		0.99
Z24	6.9	Inclusion	Picritic gabbro	38.32	0.030	40.78	0.14	0.26	19.66	0.209	99.39	78.65	1641		
Z24	6.9	Discrete crystal	Picritic gabbro	38.33	0.012	39.99	0.16	0.34	20.55	0.210	99.59	77.51	1646	7.3	0.38
Z23	8.5	Inclusion	Picritic gabbro	39.01	0.029	40.93	0.12	0.29	18.61	0.258	99.25	79.54	2031		
Z23	8.5	Discrete crystal	Picritic gabbro	38.11	0.017	40.16	0.13	0.32	20.03	0.260	99.02	78.00	2043	9.1	0.89
Z22	10.1	Inclusion	Picritic gabbro	38.35	0.045	40.87	0.15	0.31	19.50	0.238	99.47	78.78	1874		
Z22	10.1	Discrete crystal	Picritic gabbro	37.65	0.047	37.91	0.14	0.38	23.02	0.253	99.40	74.47	1987	9.3	1.03
Z25	11	Discrete crystal	Troctolite	37.23	0.026	37.98	0.22	0.37	22.87	0.269	98.97	74.67	2111	7.9	0.18
Z21	11.8	Inclusion	Picritic gabbro	38.40	0.053	40.37	0.13	0.30	19.21	0.259	98.72	77.95	2033		
Z21	11.8	Discrete crystal	Picritic gabbro	37.73	0.017	38.07	0.16	0.38	23.11	0.280	99.74	74.45	2197	8.4	0.83
Z20	13	Inclusion	Picritic gabbro	39.08	0.043	41.59	0.13	0.30	18.22	0.256	99.62	80.15	2014		
Z20	13	Discrete crystal	Picritic gabbro	38.80	0.018	38.74	0.15	0.34	21.30	0.269	99.62	76.29	2111	7.9	3.00
Z18	16	Inclusion	Picritic gabbro	38.98	0.018	41.09	0.16	0.28	18.51	0.227	99.26	79.75	1782		
Z18	16	Discrete crystal	Picritic gabbro	38.99	0.018	39.83	0.20	0.31	20.08	0.241	99.66	77.90	1897	9.1	0.40
Z17	18.5		Taxitic gabbro	*37.84*		*36.21*			*25.65*	*0.230*	*99.95*	*71.60*	*1839*		0.90
Z15	22		Taxitic gabbro	*37.10*		*32.54*			*30.28*	*0.220*	*100.16*	*65.70*	*1729*		2.93
Z11	25		Contact gabbro	*37.04*		*32.02*			*31.05*	*0.090*	*100.20*	*64.90*	*739*		1.22
Z10	27.1	Poikilitic crystal	Ol gabbro	35.84	0.000	28.19	0.26	0.48	34.82	0.058	99.65	58.97	456	8.2	1.32
Z9	29		Contact gabbro	*33.57*		*20.40*			*45.87*	*0.090*	*99.93*	*44.60*	*707*		0.64
Main Talnakh, drill core KZ1739, Severny mine[4]															
6b	1709.3		Gabbro											9.1	0.21
7b	1722	Poikilitic crystal	Ol gabbro	36.32	0.000	29.36	0.18	0.53	33.23	0.071	99.69	60.95	554		0.10
7ba	1744	Poikilitic crystal	Ol gabbro	36.61	0.003	30.70	0.19	0.52	31.79	0.086	99.91	63.05	676		0.08
7bb	1757	Poikilitic crystal	Ol gabbro	36.78	0.003	32.13	0.16	0.47	29.37	0.095	99.00	65.89	745		0.08
7c	1772.2	Poikilitic crystal	Ol gabbro	36.71	0.025	34.75	0.16	0.47	27.32	0.128	99.57	69.18	1005		0.09
8	1781	Discrete crystal	Ol gabbro	36.88	0.013	34.14	0.10	0.45	27.03	0.122	98.73	69.98	961		
9b	1790	Inclusion	Taxitic gabbro	38.82	0.032	39.89	0.10	0.33	20.61	0.200	99.98	77.36	1573		
9b	1790	Discrete crystal	Taxitic gabbro	38.23	0.012	36.97	0.12	0.37	24.10	0.175	99.98	73.05	1374		0.23
10	1792.2	Inclusion	Picritic gabbro	39.35	0.029	41.37	0.10	0.27	17.86	0.223	99.21	80.37	1754		
10	1792.2	Discrete crystal	Picritic gabbro	38.92	0.022	40.26	0.14	0.31	19.63	0.232	99.52	78.41	1825	9.6	2.28
14	1814.5	Inclusion	Picritic gabbro	38.34	0.029	39.37	0.11	0.32	20.49	0.248	98.91	77.25	1949		
14	1814.5	Discrete crystal	Picritic gabbro	36.43	0.012	34.44	0.15	0.44	26.63	0.247	98.35	69.55	1938	9.0	2.06
14b	1818.5	Discrete crystal	Picritic gabbro	37.00	0.007	32.53	0.11	0.45	29.44	0.242	99.78	66.02	1899	10.3	4.96
15	1821.5	Inclusion	Taxitic gabbro	38.22	0.020	38.46	0.12	0.31	21.28	0.200	98.60	76.18	1570		
15	1821.5	Poikilitic crystal	Taxitic gabbro	36.65	0.003	34.35	0.10	0.51	27.12	0.218	98.95	69.00	1716	10.9	3.41
16	1826	Inclusion	Olivinite	39.52	0.008	42.72	0.16	0.27	17.33	0.146	100.16	81.40	1146		
16	1826	Discrete crystal	Taxitic gabbro	38.19	0.034	36.44	0.11	0.39	25.08	0.177	100.41	71.93	1390	11.0	3.08
16bb	1832	Poikilitic crystal	Taxitic gabbro	36.30	0.002	29.67	0.17	0.70	32.90	0.249	99.98	61.30	1958	11.0	9.85
17	1846.2	Inclusion	Ol gabbro	38.75	0.013	39.55	0.15	0.34	20.53	0.125	99.45	77.30	980		
17	1846.2	Discrete crystal	Ol gabbro	37.49	0.006	34.30	0.25	0.48	26.58	0.101	99.22	69.55	796		0.41
17b	1848.4	Discrete crystal	Contact gabbro	38.15	0.005	36.95	0.13	0.43	24.15	0.134	99.95	72.95	1056	10.7	
18	1850.8		Contact gabbro											12.6	

TABLE 2. *(Cont.)*

Sample no.	Depth or distance (m)	Type of olivine	Rock type	Olivine composition[1] (wt %) SiO_2	Cr_2O_3	MgO	CaO	MnO	FeO	NiO	Total	Forsterite (mol %)	Ni in Ol (ppm)	Sulfides $\delta^{34}S$	Whole rock S^2 (wt %)
NW Talnakh, drill core 5536, Komsomolsky mine[5]															
K61	0.53	Poikilitic crystal	Ol gabbro	37.93	0.004	34.92	0.22	0.41	25.86	0.134	99.48	70.55	1054	11.1	0.12
K60	2.5	Inclusion	Taxitic gabbro	39.27	0.051	42.53	0.21	0.27	17.07	0.237	99.63	81.62	1860		
K60	2.5	Discrete crystal	Taxitic gabbro	38.85	0.020	41.81	0.24	0.29	17.86	0.255	99.32	80.68	2002	12.0	1.06
K59	3.5	Inclusion	Olivinite	39.70	0.021	42.97	0.19	0.28	17.14	0.273	100.58	81.69	2143		
K59	3.5	Discrete crystal	Taxitic gabbro	39.20	0.014	41.36	0.21	0.32	18.55	0.290	99.95	79.84	2281	11.2	
K58	5	Inclusion	Taxitic gabbro	39.71	0.026	43.41	0.21	0.26	15.99	0.262	99.87	82.87	2062		
K58	5	Discrete crystal	Taxitic gabbro	39.35	0.041	42.17	0.26	0.22	17.92	0.252	100.33	81.01	1984	10.2	2.55
K57	6	Poikilitic crystal	Taxitic gabbro	38.49	0.003	38.52	0.22	0.42	21.36	0.259	99.27	76.15	2034	11.2	
K56	8		Picritic gabbro											12.2	
K55	9	Inclusion/Pl core	Taxitic gabbro	39.45	0.016	42.62	0.21	0.29	16.84	0.268	99.68	81.91	2114		
K55	9	Inclusion/Pl rim	Taxitic gabbro	39.07	0.009	40.44	0.21	0.34	19.24	0.269	99.58	78.86	2127		
K55	9	Discrete crystal	Taxitic gabbro	38.88	0.003	39.09	0.20	0.39	20.93	0.274	99.77	76.77	2158	11.1	
K54	10.5	Poikilitic	Picritic gabbro	39.76	0.025	43.22	0.21	0.27	16.06	0.258	99.81	82.74	2027		
K54	10.5	Discrete crystal	Picritic gabbro	39.39	0.016	41.57	0.23	0.32	17.81	0.289	99.64	80.60	2267	11.3	1.42
K53	12.5	Inclusion	Taxitic gabbro	39.24	0.031	41.43	0.35	0.34	18.26	0.183	99.83	80.11	1439		
K53	12.5	Discrete crystal	Taxitic gabbro	38.72	0.000	39.34	0.25	0.43	20.70	0.183	99.62	77.11	1435	11.3	
K40	16.5	Poikilitic crystal	Taxitic gabbro	38.70	0.012	39.92	0.36	0.40	21.24	0.165	100.80	77.06	1299	11.7	
K43	20.5	Poikilitic crystal	Taxitic gabbro	37.92	0.006	36.11	0.18	0.49	24.20	0.203	99.12	72.47	1597	11.0	
K44	23.5	Inclusion	Olivinite	39.12	0.035	41.04	0.18	0.31	19.22	0.172	100.07	79.12	1353		
K44	23.5	Inclusion	Picritic gabbro	39.29	0.020	41.61	0.13	0.28	18.26	0.159	99.74	80.14	1248		
K44	23.5	Poikilitic crystal	Picritic gabbro	37.88	0.031	38.71	0.17	0.34	22.34	0.187	99.66	75.42	1472	12.0	
K45	26.5		Taxitic gabbro											11.1	
K46	29		Taxitic gabbro											11.3	
K47	31		Taxitic gabbro											11.2	
NW Talnakh, Oktyabr'sky mine[6]															
Sample no.	Drill core														
16	KZ589	Inclusion/ dark BSE image	Picritic gabbro	39.51	0.021	44.36	0.31	0.29	15.54	0.145	100.17	83.67	1140		
16	KZ589	Inclusion/ light BSE image	Picritic gabbro	38.54	0.007	40.25	0.32	0.53	20.28	0.146	100.09	77.85	1149		
16	KZ589	Discrete crystal	Picritic gabbro	38.75	0.015	40.74	0.25	0.55	19.69	0.148	100.14	78.48	1165	12.6	
11	KZ806	Inclusion/ dark BSE image	Olivinite	39.05	0.093	42.18	0.22	0.32	17.85	0.139	99.86	80.78	1091		
11	KZ806	Inclusion/ light BSE image	Olivinite	38.58	0.032	40.87	0.22	0.38	19.56	0.131	99.78	78.74	1032		
11	KZ806	Discrete crystal	Picritic gabbro	38.00	0.026	39.16	0.25	0.43	21.62	0.117	99.61	76.25	919	13.2	
Main Talnakh, drill core KZ1739, Severny mine															
2	KZ1739/1667	Poikilitic crystal	Ol gabbro	38.42		38.69	0.02	0.40	21.85	0.084	99.46	75.62	664	7.0	

[1] Values in italics are unpublished data from A. J. Naldrett
[2] Values are unpublished data from A. J. Naldrett
[3] Numbers are distances from the end of drill hole, which ended in picritic gabbro unit; this hole was drilled from an underground shaft
[4] Numbers are depths from surface
[5] Number are distances from the end of this drill hole, which ended in olivine gabbro unit; this hole was drilled from an underground shaft
[6] These holes were drilled from surface

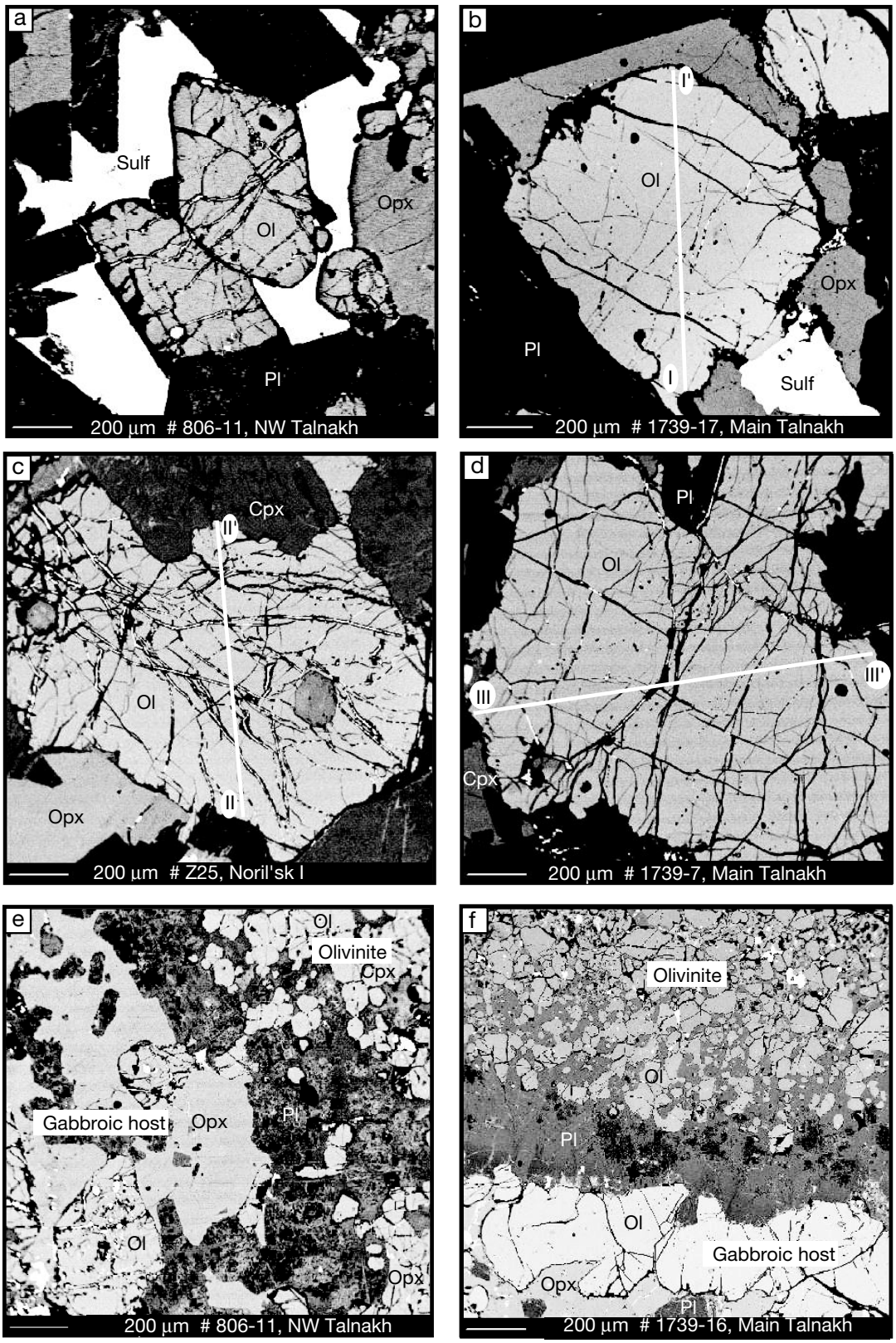

FIG. 4. BSE images showing representative textural relationships of olivine with other phases in olivine gabbro and olivinite. (a). Euhedral olivine grains with interstitial sulfide. (b), (c), and (d). Poikilitic olivine with pyroxene and plagioclase. (e) and (f). Olivinite inclusion in picritic gabbro host. The contact of an olivinite inclusion with its gabbroic host is often annealed by large plagioclase crystals that grew either parallel (e) or perpendicular (f) to the contact. Cpx = clinopyroxene, Sulf = sulfide. Other keys are the same as in Figure 3.

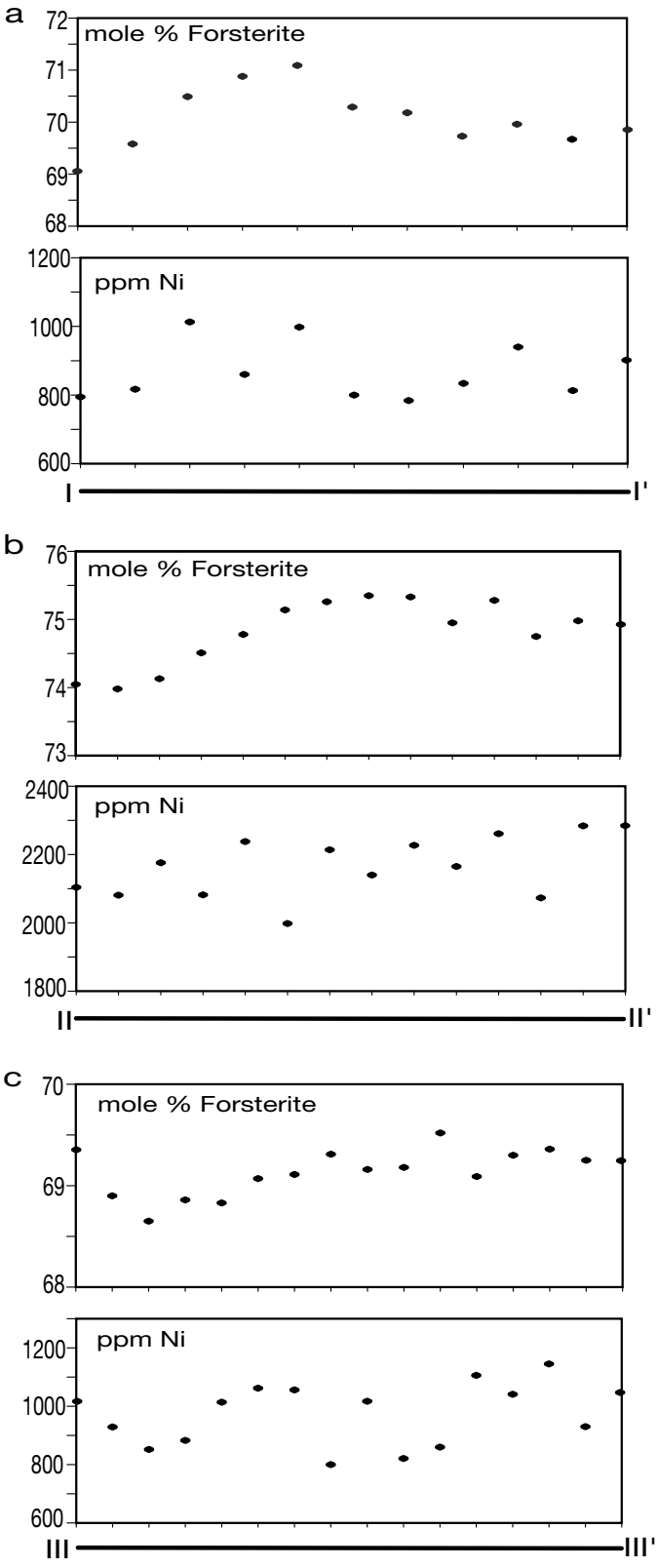

FIG. 5. Compositional traverses across poikilitic olivine crystals. The locations of the traverses are shown in Figure 4.

olivine crystals sometimes overlap, but olivine inclusions generally contain higher Fo contents (by up to 6 mol %, Fig. 6a-f). Olivine inclusions also contain more Ni than coexisting discrete olivine crystals in sulfide-poor samples (<0.3 wt % sulfur, Fig. 6a, b). These relationships are consistent with the interpretation that olivine inclusions are cumulus and coexisting discrete olivine crystals are intercumulus (see discussion section below). In sulfide-bearing samples (>0.3 wt % sulfur), however, discrete olivine crystals have Ni contents similar to or notably higher than coexisting olivine inclusions (Fig. 6c-f). In addition, some of these sulfide-bearing samples exhibit weak negative Ni-Fo correlation (Fig. 6c and e). This relationship is characteristic of subsolidus reequilibration of olivine with trapped sulfide liquid (see discussion section below).

The difference in olivine composition between olivinite and its host rock (Fig. 6g, h) is similar to the difference between olivine inclusions and coexisting discrete olivine crystals in sulfide-bearing samples. Olivine crystals in the host rock are usually more fractionated (lower Fo contents) and contain more Ni (Fig. 6g, h). In contrast, olivine crystals in olivinite are characterized by weak positive Ni-Fo correlation (Fig. 6g) or no correlation (Fig. 6h).

Stratigraphic variations of olivine and sulfur isotopes

Data from three drill cores examined in this study indicate that there are significant discontinuities in olivine compositions, particularly Ni contents, between different rock units in the Noril'sk I, Main and Northwestern Talnakh intrusions. These differences are coupled with abrupt changes (up to 2.5‰) in the isotopic composition of coexisting sulfides in the Noril'sk I and Main Talnakh intrusions but not in the Northwestern Talnakh intrusion.

Figure 7 illustrates the stratigraphic variation of olivine compositions and the isotopic compositions of sulfides in drill core 3010 located in the Zapolyarny mine in the southern part of the Noril'sk I intrusion. This hole was drilled from an underground shaft and intercepted the lower part of the intrusion through contact gabbro, olivine gabbro, taxitic gabbro, and picritic gabbro. Both contact gabbro and olivine gabbro units are sulfide poor but locally contain disseminated sulfides or sulfide veinlets. Olivine in these two units has similar compositions, containing Fo less than 67 mol percent and Ni less than 750 ppm. Olivine in the taxitic gabbro unit has slightly higher Fo content and appears to extend the trend of the underlying olivine gabbro. However the contents of Ni in olivine in the taxitic gabbro unit are much higher, ranging between 1,700 and 1,900 ppm. In the picritic gabbro, olivine inclusions have Fo contents up to 81 mol percent. The variation in the contents of Fo in olivine inclusions from this unit is rather small, mostly less than 3 mol percent. The contents of Fo in discrete olivine crystals are several mole percent less than coexisting olivine inclusions. The contents of Ni in both olivine inclusions and coexisting discrete olivine crystals display an inverse relationship with Fo contents. Olivine from a sample close to the top of the picritic unit has much lower Ni than olivine from elsewhere in this unit, which is apparently related to lower Ni content in the sulfide. The content of Ni in the sulfide portion (recalculated to 100% sulfide) of this sample is 7 wt percent. The contents

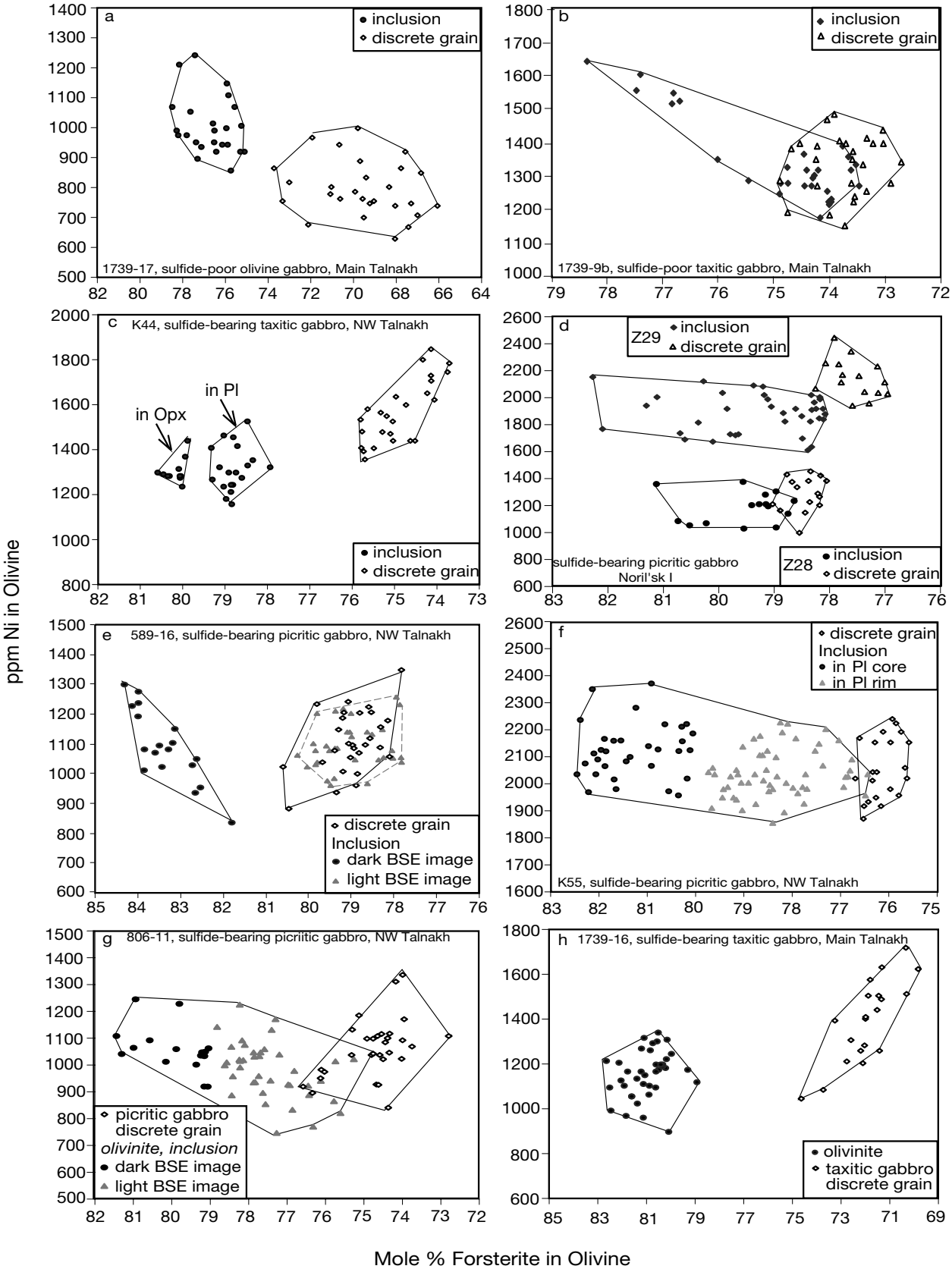

FIG. 6. Compositional relationship between different types of olivine from sulfide-poor samples (a) and (b), sulfide-bearing samples (c) to (f), and olivinite (g) and (h). See text for discussions.

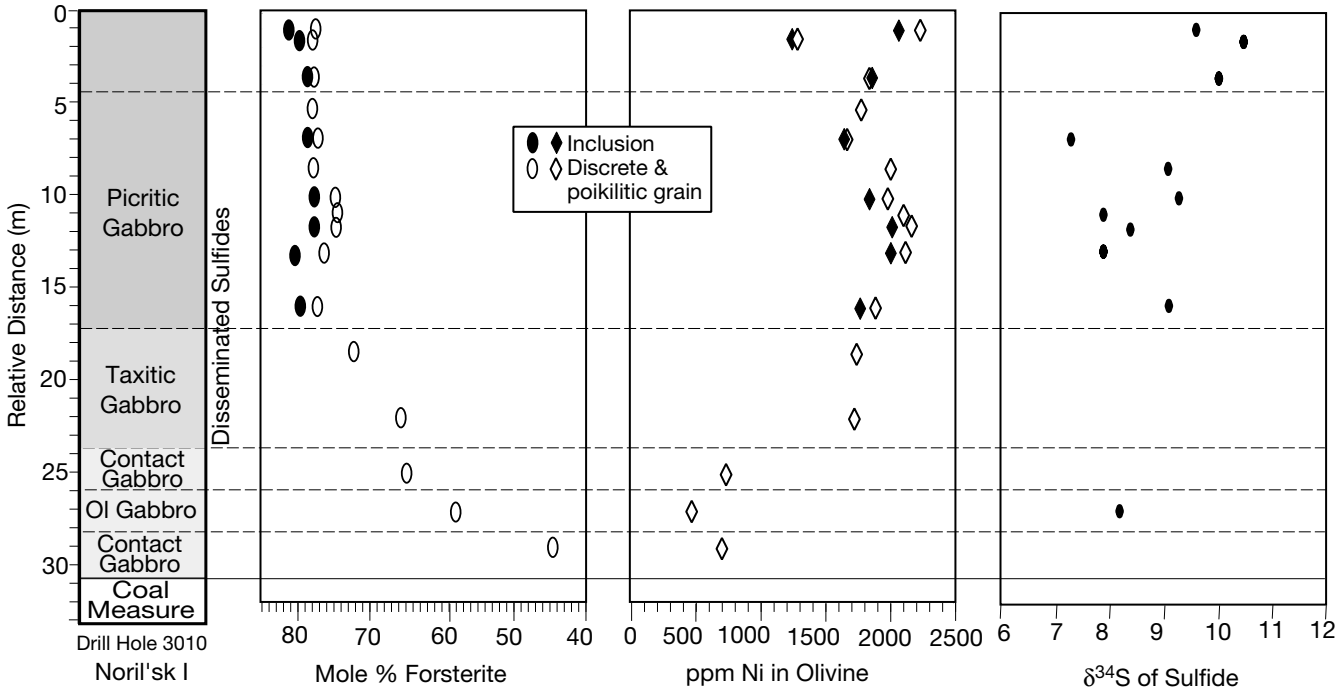

FIG. 7. Stratigraphic variations of sulfur isotope and olivine compositions in drill core 3010, Noril'sk I intrusion.

of Ni in the sulfide portion of other samples from this unit vary between 9 and 12 wt percent (A. J. Naldrett, unpub. data).

The $\delta^{34}S$ value of sulfides in the single sample analyzed from the olivine gabbro unit in this drill core is 8.2 per mil. The $\delta^{34}S$ values of sulfides in the samples from the lower part of the picritic gabbro unit vary between 7.3 and 9.3 per mil but in the upper three samples of the picritic gabbro unit they are distinctly higher, ranging from 9.6 to 10.5 per mil. This difference is notably larger than the variations of different sulfide aggregates in a single sample (typically <0.5‰).

The stratigraphic variations of olivine and the isotopic compositions of sulfides in drill core 5536 are shown in Figure 8. This hole was drilled from an underground shaft in the Komsomolsky mine in the southern part of the Northwestern Talnakh intrusion and intercepted three major rock units. From bottom to top, these are taxitic gabbro, picritic gabbro, and olivine gabbro. The olivine gabbro unit is sulfide poor, whereas the other two units contain up to 25 percent disseminated sulfides. In this drill core, the $\delta^{34}S$ values of sulfides in the samples from different rock units are similar, varying between 10.2 and 12.2 per mil, with most of the values close to 11.2 per mil. In contrast, different olivine compositions are apparent in different units. Olivine in the picritic gabbro unit is the most primitive and has the highest Ni content. Olivine in the underlying taxitic gabbro unit contains slightly less Fo and significantly less Ni. Olivine in the olivine gabbro unit is characterized by the lowest Ni content.

Figure 9 shows the stratigraphic variations of olivine and sulfur isotope compositions in drill core KZ1739 located in the Severny mine in the northern part of the Main Talnakh intrusion. This hole was drilled from surface and intercepted all major rock units of the intrusion: gabbro, upper olivine gabbro, and upper taxitic gabbro in the upper part; picritic gabbro in the middle; lower taxitic gabbro, lower olivine gabbro, and contact gabbro in the bottom. The compositions of discrete olivine in the upper and lower olivine gabbro units are similar. The contents of both Fo and Ni in olivine in the upper olivine gabbro unit decrease upward. Discrete olivine in the contact gabbro unit contains Fo and Ni contents slightly higher than discrete olivine in the overlying olivine gabbro. Olivine inclusions from different rock units have similar Fo contents, but those from the lower olivine gabbro unit contain much less Ni. The contents of Ni in both olivine inclusions and discrete olivine crystals from the picritic gabbro unit are similar, although the olivine inclusions have much higher Fo contents. The Fo and Ni contents of olivine inclusions and discrete olivine crystals in sulfide-poor samples from the lower olivine gabbro unit and upper taxitic gabbro unit are positively correlated, whereas the Fo and Ni contents in sulfide-bearing samples from the lower taxitic unit are negatively correlated. Neither relationship is evident in the picritic gabbro unit.

The $\delta^{34}S$ values of sulfides in the taxitic gabbro unit are all close to 11 per mil. The $\delta^{34}S$ values of sulfides in the picritic gabbro unit are 1 to 2 per mil lower. The $\delta^{34}S$ values in the contact gabbro unit vary between 10.7 and 12.6 per mil. A sample from the gabbro unit has a notably lower $\delta^{34}S$ value of 9.1 per mil.

Discussion

Controls on the compositional variations of olivine

The most likely influences on olivine composition include fractional crystallization and subsolidus reequilibration with interstitial silicate and trapped sulfide liquids. Nickel and

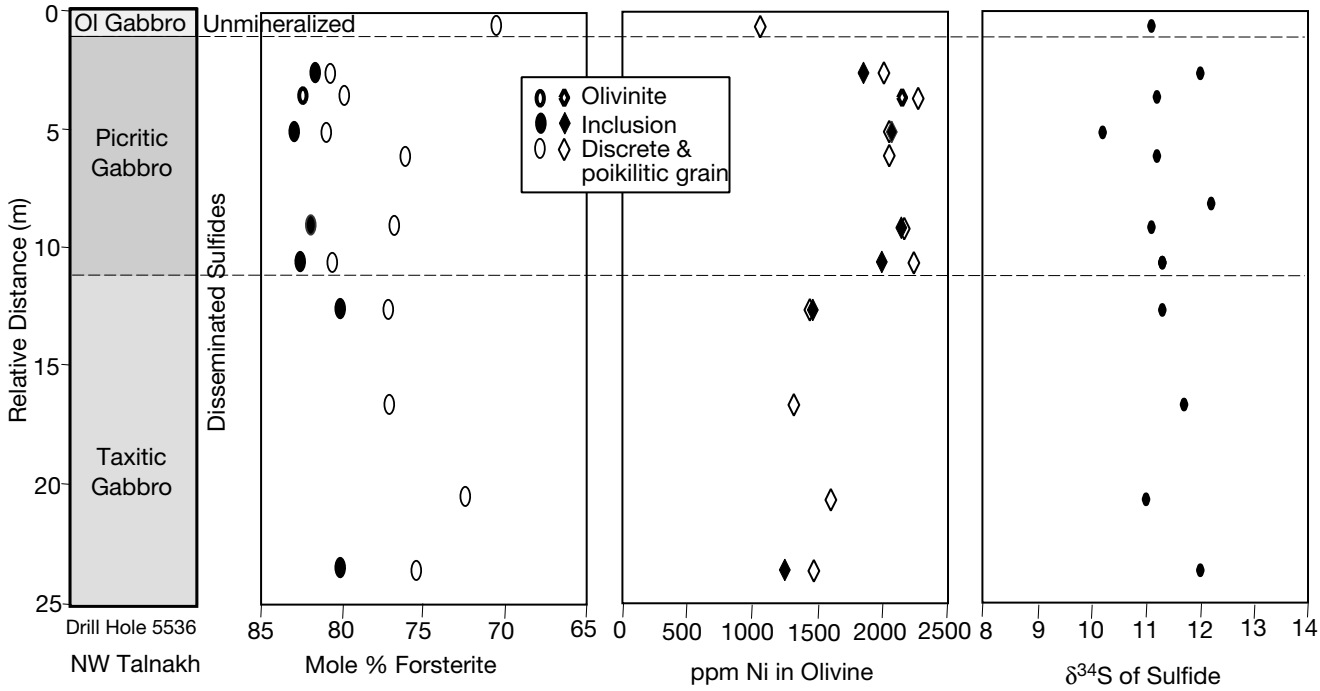

FIG. 8. Stratigraphic variations of sulfur isotope and olivine compositions in drill core 5536, Northwestern Talnakh intrusion.

magnesium are compatible in olivine and thus decrease in abundance during fractional crystallization. In contrast, iron is incompatible relative to magnesium. Thus the contents of Fo and Ni in olivine decrease during fractional crystallization.

The compositions of early cumulus olivine may be modified by subsolidus reequilibration with intercumulus silicate liquid. Olivine that crystallizes from the intercumulus silicate liquid, nucleating on a core of original cumulus olivine, will become poorer in the Fo component as the intercumulus silicate liquid fractionates further. Diffusion of iron and magnesium within the olivine structure will result in olivine with a composition that is poorer in Fo than the original cumulus material. Barnes

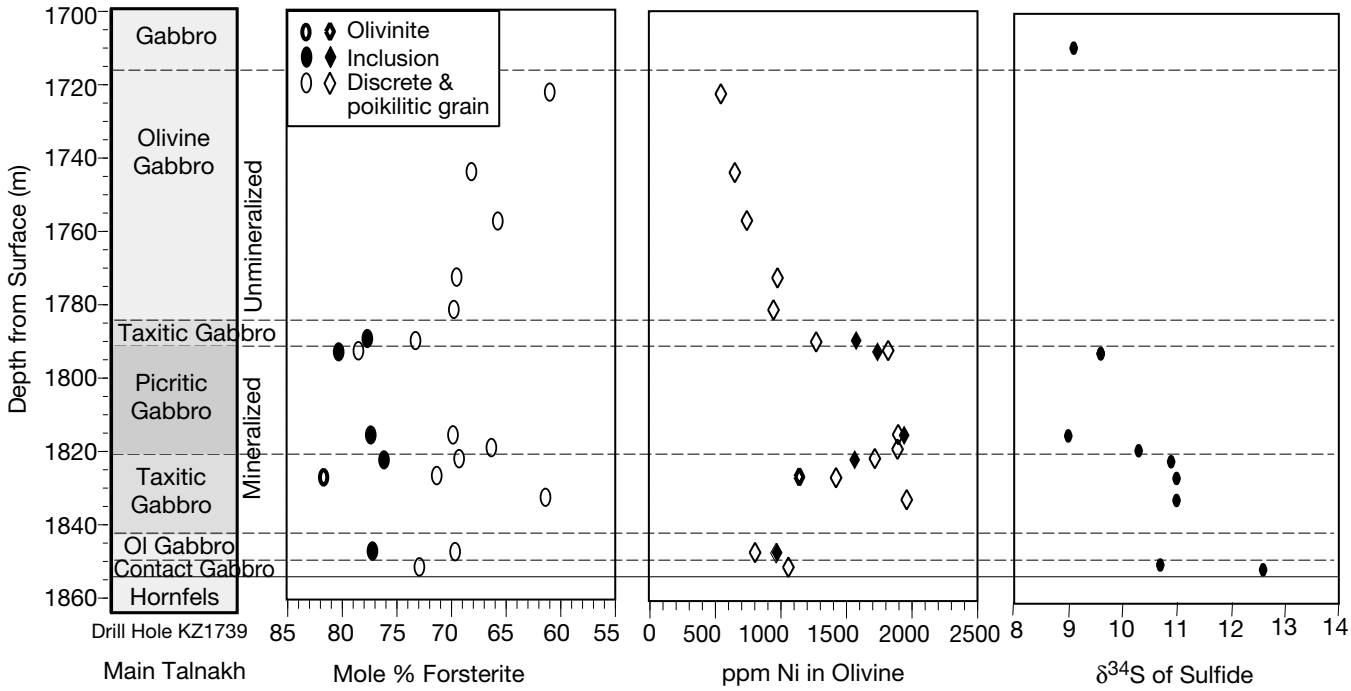

FIG. 9. Stratigraphic variations of sulfur isotope and olivine compositions in drill core 1739, Main Talnakh intrusion.

(1986, p. 524) has referred to this effect as "trapped liquid shift." Discrete and poikilitic olivine crystals are inevitably subjected to such compositional modification, resulting in lower Fo contents than their original compositions.

In contrast, the original compositions of olivine inclusions are protected by their host oikocrysts from subsequent reequilibration with intercumulus silicate liquid, so that their high Fo contents and positive Ni-Fo relationships are preserved. The positive Ni-Fo correlations are weaker or completely disappear in olivine inclusions that are associated with sulfide inclusions, which may be related to local subsolidus reequilibration with coexisting sulfide inclusions.

When olivine is immersed in a sulfide liquid, the crystal and liquid will exchange Ni and Fe according to the reaction:

$$NiO_{olivine} + FeS_{sulfide} = NiS_{sulfide} + FeO_{olivine.} \quad (1)$$

The exchange partition coefficient K_D for this reaction is defined as:

$$K_D = (NiS/FeS)_{sulfide}/(NiO/FeO)_{olivine,} \quad (2)$$

where concentrations are expressed in mole fractions. K_D is related to the equilibrium constant, K, by the expression:

$$K = K_D \times (\gamma_{NiS}/\gamma_{FeS})_{sulfide}/(\gamma_{NiO}/\gamma_{FeO})_{olivine,} \quad (3)$$

where γ refers to the activity coefficient. If Ni and Fe substitutions into olivine are ideal, as suggested by Campbell and Roeder (1968), that is $\gamma_{NiO} = 1$ and $\gamma_{FeO} = 1$, the exchange partition coefficient for the reaction will be equal to the equilibrium constant multiplied by the ratio of the activity coefficients of the two sulfide components in the sulfide liquid. Brennan and Caciagli (2000) have found that although it is insensitive to temperature, K_D varies with the Ni content of the sulfide liquid, decreasing as NiS decreases. When the Ni content of the sulfide is about 5 wt percent, $K_D = 10$. The ratio of $\gamma_{NiS}/\gamma_{FeS}$ is not constant, but is much greater than unity, and for magmatic systems in which the Ni content of the sulfide liquid is close to 5 wt percent,

$$(NiS/FeS)_{sulfide} \approx 10 \times (NiO/FeO)_{olivine.} \quad (4)$$

Therefore, when a suite of olivine crystals with varying FeO contents is immersed in a sulfide liquid, after reaction with the sulfide liquid the olivine with higher FeO content will contain more Ni than the olivine with lower FeO content. An inverse Ni-Fo relationship of olivine from individual sulfide-bearing samples is thus consistent with subsolidus reequilibration of olivine with trapped sulfide liquid.

Modeling of olivine compositional variations

The compositions of olivine from different intrusions are compared in Figure 10a-c. The model curves represent the compositional variations of olivine expected to crystallize from magmas with variable initial Ni contents and the same major element compositions during fractional crystallization. The model lines labeled *a, b,* and *c* represent initial Ni

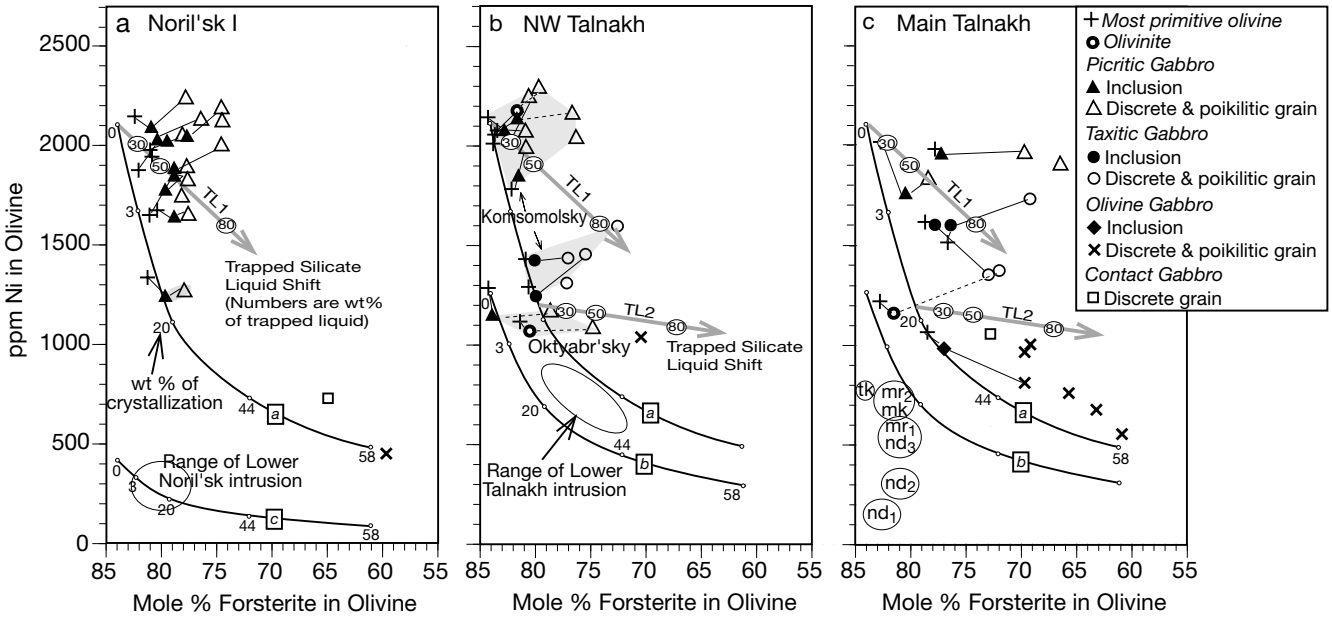

FIG. 10. Modeling of olivine fractionation. The model curves represent the compositional variations of olivine expected to crystallize from magmas with variable initial Ni contents and the same major element compositions during fractional crystallization. The model lines labeled *a, b,* and *c* represent initial Ni contents of 300, 180, and 60 ppm, respectively. The major element compositions are from the average values of the Noril'sk-type sills given by Zen'ko and Czamanske (1994b). The simulation of fractional crystallization was performed for 1 kbar at the QFM (quartz-fayalite-magnetite) buffer using the silicate liquid model MELTS of Ghiorso and Sack (1995) (JAVA version 1.1.1, 2001 provided online by M. S. Ghiorso). Olivine data for the Lower Noril'sk and Lower Talnakh intrusions are from Naldrett et al. (1992) and Duzhikov et al. (1988), respectively. Noril'sk basalts: mk = Mokulaevsky, mr_1 = Lower Morongovsky, mr_2 = Upper Morongovsky, nd_1 = Lower Nadezhdinsky, nd_2 = Middle Nadezhdinsky, nd_3 = Upper Nadezhdinsky, tk = Tuklonsky.

contents of 300, 180, and 60 ppm, respectively. The major element compositions are from the average values of the Noril'sk-type sills given by Zen'ko and Czamanske (1994b). The initial content of H_2O is assumed to be 0.2 wt percent, which is at the lower end of values shown by midocean ridge basalts (Moore, 1970). The simulation of fractional crystallization was performed for 1 kbar at the QFM (quartz-fayalite-magnetite) buffer using the silicate liquid model MELTS of Ghiorso and Sack (1995; JAVA version 1.1.1, 2001, provided online by M. S. Ghiorso). Olivine is predicted to crystallize at 1,230°C. Plagioclase joins olivine at 1,198°C. Clinopyroxene joins both olivine and plagioclase at 1,175°C (Table 3). This crystallization sequence is generally in good agreement with petrographic observation. Nickel fractionation was calculated assuming that the D^{Ni} value (concentration in solid/concentration in liquid) for olivine, clinopyroxene, and plagioclase is 7, 1, and 0, respectively. The olivine liquid D^{Ni} used here is notably lower than that of the experiments performed on sulfur-free basaltic systems, such as those by Leeman and Lindstrom (1978) and Snyder and Carmichael (1992) but is within the range of values for the midocean basalts (4.5–9.2) given by Li and Ripley (2002). The lower D^{Ni} values in the natural sulfide-bearing samples are related to the presence of some Ni as NiS in silicate liquid. The Ni of NiS is not directly available for partitioning into olivine but contributes to the liquid concentration and thus reduces the apparent D^{Ni} value calculated, based on the total Ni concentration of the liquid.

The shift in olivine compositions in the trapped silicate liquid (Fig. 10) is calculated from mass balance, using the modes and compositions of cumulus and intercumulus olivine calculated using MELTS for fractional and equilibrium crystallization, respectively. In the first example (TL1), the trapped silicate liquid crystallizes 20 percent olivine of Fo_{62}, 48 percent plagioclase, 28 percent clinopyroxene, and 4 percent spinel. In the second example (TL2), the trapped liquid crystallizes 8 percent olivine of Fo_{55}, 50 percent plagioclase, 35 percent clinopyroxene, and 7 percent spinel. The Ni in the trapped silicate liquid is assumed to partition into the silicate minerals according to their D^{Ni} values given above and a D^{Ni} value of 2 for spinel. The calculated shift of Ni content in olivine in the trapped silicate liquid is minimum value because potential sulfide segregation from the trapped silicate liquid during crystallization is not included.

Discrete and poikilitic olivine crystals have distinctly lower Fo contents than coexisting olivine inclusions (Fig. 10), consistent with the results of fractional crystallization and/or reequilibration with intercumulus silicate liquids. Higher Ni contents in discrete and poikilitic olivine than in coexisting olivine inclusions from the sulfide-bearing samples are consistent with subsolidus reaction of olivine with trapped sulfide liquids.

Compositions of olivine inclusions

In this section we focus on olivine inclusions because they have been well protected by their host oikocrysts from subsequent reequilibration with interstitial silicate and sulfide liquids, and their compositions are directly related to the compositions of their parental magmas. Olivine inclusions from the Noril'sk I and Lower Noril'sk intrusions have similar Fo

TABLE 3. Modeling of Olivine Crystallization[1]

Temperature (°C)	Solids[2] Ol : Pl : Cpx	Liquid (wt %)	Liquid composition (in wt %)										Olivine composition[3]			
			SiO_2	TiO_2	Al_2O_3	Fe_2O_3	FeO	MnO	MgO	CaO	Na_2O	K_2O	P_2O_5	H_2O	Fo	Ni[a]	Ni[b]	Ni[c]
1230	1 : 0 : 0	100	48.20	1.05	16.32	1.74	9.65	0.19	8.93	10.47	2.35	0.75	0.13	0.20	84	2100	1260	420
1200	1 : 0 : 0	97.2	48.56	1.09	16.81	1.76	9.50	0.18	7.87	10.77	2.42	0.78	0.13	0.21	82.4	1721	1033	344
1198	1 : 2.5 : 0	96.7	48.48	1.09	16.80	1.77	9.52	0.19	7.80	10.78	2.43	0.78	0.13	0.21	82.1	1660	996	332
1180	1 : 2.8 : 0	81.9	48.95	1.29	15.52	1.97	10.46	0.20	7.11	10.62	2.56	0.91	0.16	0.24	79.7	1190	713	236
1177	1 : 2.6 : 0	79.8	49.03	1.32	15.31	2.01	10.60	0.20	7.03	10.59	2.58	0.92	0.16	0.25	79.2	1134	680	227
1175	1 : 4.3 : 3.8	78.2	49.05	1.35	15.23	2.03	10.73	0.20	6.91	10.52	2.60	0.95	0.17	0.25	79	1108	663	219
1160	1 : 4 : 3.3	66.6	49.13	1.55	14.89	2.19	11.77	0.23	6.14	9.68	2.82	1.10	0.19	0.30	76	906	545	178
1140	1 : 3.7 : 2.8	55.6	49.23	1.82	14.41	2.39	13.01	0.26	5.22	8.71	3.06	1.30	0.23	0.36	72	731	442	142
1120	1 : 3.4 : 2.2	47.8	49.32	2.07	13.92	2.56	14.10	0.29	4.40	7.91	3.25	1.49	0.27	0.42	67	590	357	113
1100	1: 3.5 : 1.75	41.7	49.41	2.32	13.42	2.73	15.05	0.31	3.66	7.23	3.41	1.68	0.31	0.48	61	485	295	92

[1] Initial magma composition is assumed to be the same as the average composition of the Noril'sk-type sills from Zen'ko and Czamanske (1994b)

[2] Results of fractional crystallization calculated at 1 kbar, QFM buffer, 0.2 wt % H_2O, and 1°C increment using MELTS of Ghiorso and Sack (1995); Cpx = clinopyroxene, Pl = plagioclase, Ol = olivine

[3] Models *a*, *b*, and *c* are calculated assuming that Ni in initial magma is 300, 180, and 60 ppm, respectively; D^{Ni} for Ol, Pl, and Cpx is assumed to be 7, 0, and 1, respectively

contents (Fig. 10a) but strikingly different Ni contents, which require different initial Ni contents in their parental magmas (300 ppm, line *a* vs. 60 ppm, line *c*). It is seen that 5 percent crystallization in accordance with the model of 300 ppm initial Ni in magma accounts well for the most primitive olivine inclusions from the Noril'sk I intrusion, except for one sample which has a much lower Ni content and falls closer to the model line at about 20 percent of crystallization.

Compared to the Noril'sk I intrusion, the contents of Fo in olivine inclusions from the picritic gabbro unit in the Komsomolsky mine in the Northwestern Talnakh intrusion are slightly higher (Fig. 10b). Most olivine inclusions from this unit fall closer to the model of 300 ppm initial Ni in magma at about 5 percent crystallization. Olivine inclusions from the taxitic gabbro unit in the Komsomolsky mine in the Northwestern Talnakh intrusion are more fractionated and fall near the model line between 10 and 12 percent crystallization. Olivine inclusions from the picritic gabbro unit in the Oktyabr'sky mine in the Northwestern Talnakh intrusion have significantly lower Ni contents than those from the same type of rock in the Komsomolsky mine in the same intrusion and require a much lower initial Ni content in their parental magma (180 ppm, line *b*).

In the Main Talnakh intrusion, the most primitive olivine inclusion from the picritic gabbro unit falls near the model line of 300 ppm initial Ni in magma at about 2 percent crystallization (Fig. 10c). Other olivine inclusions from the picritic gabbro unit are displaced to the right, suggesting more evolved magma compositions. Olivine inclusions from the olivine gabbro unit plot close to the model line at about 22 percent crystallization.

In the Northwestern Talnakh intrusion, the compositions of olivine in olivinite xenoliths are similar to that of olivine inclusions in the host rocks of the xenoliths (Fig. 10b), suggesting an in situ origin for the xenoliths. In the Main Talnakh intrusion, however, the compositions of olivine in olivinite xenoliths are distinctly different from that of olivine inclusions in the matrix, suggesting a different or external origin for the xenoliths.

Comparison of observed with modeled olivine compositions (Fig. 10) indicates that at least three different parental magmas of similar FeO and MgO but distinctly different Ni contents (i.e., magmas *a, b,* and *c*) are required to explain the compositions of olivine inclusions from the ore-bearing and related intrusions in the Noril'sk-Talnakh area. The Lower Noril'sk intrusion is inferred to have formed from a distinctly Ni-depleted magma (i.e., magma *c,* Ni depleted relative to magma *a*). The magma of the Lower Talnakh intrusion is inferred to be slightly less depleted in Ni than the magma of the Lower Noril'sk intrusion. The picritic gabbro unit of the Noril'sk I intrusion is inferred to have crystallized from a Ni-undepleted magma (i.e., magma *a*). In both the Main and Northwestern Talnakh intrusions, different magmas (i.e., magmas *a* and *b*) were involved in the formation of the picritic gabbro unit in different localities within each intrusion. The inferred parental magmas of the associated contact gabbro, olivine gabbro, and taxitic gabbro units in the Noril'sk I, Main and Northwestern Talnakh intrusions are similar to the fractionated liquids of magma *a* or *b,* but the abrupt changes in the composition of olivine with depth in these intrusions suggest that the fractionation did not take place in situ but rather at depth.

Link between intrusions and lavas

On the basis of experimental data for the partitioning of PGE between sulfide and silicate melts, Naldrett et al. (1992, 1995, 1996) estimated that the PGE contents of the ores in the Noril'sk I and Talnakh intrusions must have been derived from about 50 × more magma than the amount of magma that is represented in each intrusion. They proposed that the intrusions were lava conduits through which much of the magmas involved were erupted to surface. Their latest model (Naldrett and Lightfoot, 1999) is summarized below. The nd_{1-2} magma was produced in a deep-level chamber by fractionation and contamination of the tk magma with granodioritic crust. This contaminated magma lost much of its Ni, Cu, and PGE through precipitation of sulfide liquid that resulted from contamination. The nd_{1-2} magma was then pushed up by successive surges of new magma to a higher level close to the surface, where further fractionation and additional removal of sulfide liquids occurred. The sulfide liquids became trapped in the exit conduits to this chamber, which were the immediate feeder channels for the volcanism. This is thought to have involved assimilation of evaporite-bearing sediments and further sulfur saturation. Following eruption of the nd_2, new magma of mr_2-mk type entered the high-level magma chamber in a series of pulses and mixed with the resident sulfide-bearing magma before erupting to form the nd_3 and mr_1 lavas.

Using the silicate liquid model MELTS (Ghiorso and Sack, 1995) and the average composition of each of the lavas referred to above, only the tk lava is predicted to be capable of crystallizing olivine (Fo_{85}) similar to the most primitive olivine from the intrusions (Table 1). The other lavas are not expected to crystallize olivine under variable pressures ranging from atmosphere to mantle conditions primarily due to their high SiO_2 contents. Using a constant olivine liquid Fe-Mg exchange coefficient $(FeO/MgO)_{olivine}/(FeO/MgO)_{magma}$ of 0.3 (this value has been proved to be insensitive to composition and temperature in basaltic systems by the experiments of Roeder and Emslie, 1970), the Fo and Ni contents of olivine that may crystallize from these lavas would be less than 83 mol percent and 700 ppm, which are, respectively, slightly and significantly lower than these variables in olivine inclusions in the ore-bearing intrusions.

It should be pointed out that there are uncertainties related to the use of average compositions of the lava formations in the above calculations. Deviations of MgO, FeO, and Ni contents in different samples from a single formation are up to 8, 6, and 30 percent, respectively (Lightfoot et al., 1994). The above calculations nevertheless indicate that the lavas from the Nadezhdinsky to Morongovsky Formations that were previously thought to be comagmatic with the ore-bearing intrusions (e.g., Naldrett and Lightfoot, 1999) are generally more fractionated than the magmas from which the olivine inclusions in the intrusions crystallized. This difference may have resulted from further olivine crystallization prior to final eruption, but Latypov (2002) has shown that the lavas and the intrusive rocks cannot be related through fractional crystallization. Wooden et al. (1992) and Czamanske et al. (1994,

1995) have shown that there are small variations (~5% difference) in Sr and Pb isotope compositions between the lavas and intrusive rocks. In addition, the $\delta^{34}S$ values of the lavas are up to 10 per mil lower than the $\delta^{34}S$ values of the sulfide ores in ore-bearing intrusions (Ripley et al., in press).

Possible mechanisms of contamination by crustally derived sulfur

The very high $\delta^{34}S$ values of the sulfides (8–14‰) from the Noril'sk I, Northwestern and Main Talnakh intrusions relative to typical mantle sulfur ($\delta^{34}S$ value of 0 ± 3‰) have been attributed to contamination with ^{34}S-enriched crustally derived sulfur (e.g., Grinenko, 1985) or to an extreme of mantle heterogeneity (e.g., Wooden et al., 1992). New analyses of two sulfide-poor gabbroic samples (<550 ppm sulfur) from the central part of the Northwestern Talnakh intrusion (drill core KZ1812) yield $\delta^{34}S$ values of 1.5 and 3.6 per mil. These values are similar to the values of the sulfide-poor rocks (<1,000 ppm sulfur) from other intrusions in the area (Grinenko, 1985) and illustrate the fact that high sulfur contents couple with increasing $\delta^{34}S$ values. It is difficult to imagine that only the sulfur-rich rocks in the Noril'sk-Talnakh area would record a mantle source characterized by anomalous $\delta^{34}S$ signatures. The data are much more consistent with addition to the magmas of crustally derived ^{34}S-enriched sulfur.

Although in situ assimilation of country-rock sulfur via partial melting of evaporites could have occurred in the Main and Northwestern Talnakh intrusions that intruded within evaporite-bearing sediments, this would not have been possible in the Noril'sk I intrusion because this intrusion was emplaced some 500 m above the available evaporite strata. Furthermore, the probability of melting gypsum or anhydrite (melting point of 1,425°C) by the other intrusions deserves careful consideration. Potential fluxes which may act to lower the melting point of anhydrite have not been discovered. Dissolution of evaporites by sulfur-undersaturated basaltic magmas would be expected in response to chemical potential gradients, but such a process may be too slow for efficient sulfide saturation. Another possibility involves the leaching of sulfates by hydrothermal fluids and diffusive transfer of sulfur via the fluid phase. Leaching of sulfates by circulating hydrothermal fluids has been called upon for hydrothermal ore deposition in many environments (e.g., Casadevall and Ohmoto, 1977; Janecky and Shanks, 1988). Heat associated with the voluminous magmatism in the Noril'sk-Talnakh area certainly initiated fluid flow in the crust, and the interaction of evaporites and hydrothermal fluids could have led to the generation of sulfur-bearing brines during magma emplacement. Partial reduction of the sulfate in the hydrothermal fluid via reaction with reductants, such as the coal measures in the area, could have led to reduced sulfur with $\delta^{34}S$ values of about 15 per mil and oxidized sulfur with $\delta^{34}S$ values of greater than 20 per mil. Such diffusive transfer of sulfur via fluids may be a viable alternative to partial melting or dissolution of the evaporates by magma.

Assuming a $\delta^{34}S$ value of 18 per mil for the average value of sulfur from the fluids (this value is between that of the reduced and oxidized sulfur referred to above) and the mantle-derived magma contained 800 ppm sulfur (similar to the values of the chilled marginal rocks of the Bushveld Complex; Davies and Tredoux, 1985) with a $\delta^{34}S$ value of 1 per mil (similar to the lower end of values of the unmineralized intrusions in the Noril'sk-Talnakh area; Grinenko, 1985), a simple mixing calculation indicates that the addition of 900 ppm sulfur from the fluids to the magma would yield $\delta^{34}S$ of 10 per mil in the contaminated magma and that the resulting contaminated magma would have contained 1,700 ppm sulfur. Using the equation of Li et al. (2001), the solubility of sulfur in the magma is estimated to be 1,500 ppm, assuming the composition of this magma resembled the average composition of the Noril'sk-type sills given by Zen'ko and Czamanske (1994b). The content of sulfur in this magma exceeds its solubility by 200 ppm and an immiscible sulfide liquid (~0.05 wt % FeS) would have segregated. For the purpose of comparison, we refer to this type of sulfide as early sulfide. The R value for the early sulfide is 2,000. If the amount of sulfur added to the magma from the fluids is reduced by 100 ppm, the contaminated magma would yield $\delta^{34}S$ of 9.8 per mil and 100 ppm excess sulfur, and the R value for the early sulfide would be 4,000.

If the system remained closed after initial sulfide segregation, the remaining 1,500 ppm sulfur in the magma would have eventually segregated from the magma during cooling and crystallization. For the purpose of comparison, we refer to this type of sulfide as late sulfide. Both the early and late sulfide liquids would have the same $\delta^{34}S$, but the later would be characterized by much lower chalcophile element concentrations because of its relatively low R value. The average R value for the late sulfide would be only about 200. Mixing of both sulfide liquids would have produced a final sulfide liquid containing much less PGE than the early sulfide.

In an open system, however, the magma may leave the early sulfide in the conduit as it continues to travel to higher levels. In this case metal dilution of the early sulfide by the late sulfide would be avoided and the sulfide left in the conduit would have the original high PGE concentrations as well as elevated $\delta^{34}S$ values.

As shown above, the early sulfide segregated in response to slightly different amounts of contamination would have similar isotope compositions but different PGE concentrations due to different R values. In the Komsomolsky mine in the Northwestern Talnakh intrusion, the bulk sulfide in the picritic gabbro and olivine gabbro units has significantly different Pd contents (>10 vs. <5 ppm in recalculated 100% sulfide; A. J. Naldrett, unpub. data) and similar $\delta^{34}S$ values (close to 11.2‰), which can be interpreted in terms of different amounts of contamination.

It should be pointed out that the above mass-balance calculations are highly generalized because contamination, sulfide segregation, and magma mixing may occur simultaneously or continuously. In addition, there are uncertainties associated with the parameters used in the above calculations. Nevertheless, the results demonstrate that the sulfide ores in the ore-bearing intrusions could have formed via addition of sulfur from circulating fluids to sulfur-undersaturated, chalcophile element-undepleted magma traveling through open conduits. Much of the early magma may have intruded to form the voluminous peripheral sills of the ore-bearing intrusions rather than being erupted to form lavas.

Conclusions

Our data indicate that the different rock units in the Noril'sk I, Main and Northwestern Talnakh intrusions are not related to each other via in situ differentiation of a common parental magma but rather are consistent with separate pulses of magma with variable degrees of differentiation, possibly involving olivine crystallization and assimilation of siliceous crustal material in a staging chamber. The crustal isotopic signature (i.e., high $\delta^{34}S$ values) and high PGE concentrations of the sulfide are best explained by segregation of immiscible sulfide liquid in response to the addition of ^{34}S-enriched crustal sulfur via circulating fluids to a sulfur-undersaturated and chalcophile element-undepleted magma in a dynamic conduit. In this model, the immiscible sulfide droplets settled down to the base of the wider parts of the conduit as the magma continued to ascend to higher levels. Successive pulses of new magma entered the conduit, reacted with the early sulfide, and displaced much of the early magma in the conduit, similar to the situations at the Voisey's Bay Ni-Cu deposit, Labrador (Li et al., 2000) and the Uitkomst Ni-Cu deposit, South Africa (Li et al., 2002). The ore-bearing intrusions are thought to represent the wider parts of the conduits and their voluminous, sulfide-poor peripheral sills represent some (if not all) of the magmas that flowed out of the conduits.

Acknowledgments

We are indebted to V. Fedorenko and P. Lightfoot for direct and indirect contribution of some of the samples used in this study and for their constructive comments to an earlier draft of this paper. The clarity of the manuscript has benefited from helpful comments by G. Czamanske, as well as thorough reviews by M. Burnham, J. Mungall, a member of the editorial board, and the editor. We would like to thank Dongbok Shin for his assistance in sulfur isotope analysis. Partial support for this work was provided through an NSF grant EAR 0104580 to C. Li and E.M. Ripley.

May 14, September 4, 2002

REFERENCES

Barnes, S.J., 1986, The effect of trapped liquid crystallization on cumulus mineral compositions in layered intrusions: Contributions to Mineralogy and Petrology, v. 93, p. 524–531.

Brenan, J.M., and Caciagli, N.C., 2000, Fe-Ni exchange between olivine and sulfide liquid: Implications for oxygen barometry in sulfide-saturated magmas: Geochimica et Cosmochimica Acta, v. 64, p. 307–320.

Brügmann, G.E., Naldrett, A.J., Asif, M., Lightfoot, P.C., Gorbachev, N.S., and Fedorenko, V.A., 1993, Siderophile and chalcophile metals as tracers of the evolution of the Siberian trap in the Noril'sk region, Russia: Geochimica et Cosmochimica Acta, v. 57, p. 2001–2018.

Campbell, F.E., and Roeder, P.P., 1968, The stability of olivine and pyroxene in the Ni-Mg-Si-O system: American Mineralogist, v. 53, p. 257–258.

Campbell, I.H., and Naldrett, A.J., 1979, The influence of silicate:sulfide ratios on the geochemistry of magmatic sulfides: Economic Geology, v. 74, p. l503–l505.

Casadevall, T.J., and Ohmoto, H., 1977, Sunnyside mine, Eureka mining district, San Juan County, Colorado: Geochemistry of gold and base metal ore deposition in a volcanic environment: Economic Geology, v. 72, p. l285–l320.

Czamanske, G.K., 2002, Petrographic and geochemical characterization of ore-bearing intrusions of the Noril'sk-type, Siberia: With discussion of their origin, including additional datasets and core logs: U.S. Geological Survey Open-File Report 02-74, available on the web: http://geopubs.wr.usgs.gov/open-file/of02-74/.

Czamanske, G.K, Wooden, J.L., Zientek, M.L., Fedorenko, V.A., Zen'ko, T.E., Kent, J., King, B-S.W., Knight, R.J., and Siems, D.F., 1994, Geochemical and isotopic constraints on the petrogenesis of the Noril'sk Talnakh ore-forming system: Ontario Geological Survey Special Publication 5, p. 313–342.

Czamanske, G.K., Zen'ko, T.E., Fedorenko, V.A., Calk, L.C., Budahn, J.R., Bullock, J.H., Jr., Fries, T.L., King, B-S.W., and Siems, D.F., 1995, Petrographic and geochemical characterization of ore-bearing intrusions of the Noril'sk type, Siberia: With discussion of their origin: Resource Geology Special Issue 18, p. 1–48.

Davies, G., and Tredoux, M., 1985, The platinum-group element and gold contents of the marginal rocks and sills of the Bushveld Complex: Economic Geology, v. 80, p. 838–848.

Distler, V.V., Genkin, A.D., and Duzhihov, O.A., 1986, Sulfide petrology and genesis of copper-nickel ore deposits, *in* Freidrich, G.H., Genkin, A.D., Naldrett, A.J., Ridge, J.D., Sillitoe, R.H., and Vokes, F.M., eds., Geology and metallogeny of copper deposits: Heidelberg, Berlin, Springer-Verlag, p. 111–123.

Duzhikov, O.A., Distler, V.V., Strunin, B.M., Mkrtychjan, A.K., Cherman, M.L., Sluzhenikin, S.F., and Lurje, A.M., 1988, Geology and metallogeny of the sulfide deposits of the Noril'sk region: Moscow, Nauka, 278 p. (in Russian).

——1992, Geology and metallogeny of the sulfide deposits of the Noril'sk region, USSR: Society of Economic Geologists Special Publication 1, 242 p. (English translation of 1988 Russian edition).

Fedorenko, V.A., 1981, Petrochemical series of volcanic rocks of the Noril'sk region: Geology and Geophysics, v. 6, p. 78–88 (in Russian).

——1994, Evolution of magmatism as reflected in the volcanic sequence of the Noril'sk region: Ontario Geological Survey Special Publication 5, p. 171–184.

Fedorenko, V.A., Stifeyeva, G.T., Makeyeva, L.V., Sukhareva, M.S., and Kuznetsova, N.P., 1984, The basic and alkali-basic intrusions of the Noril'sk area in relation to their comagmatism with effusive formations: Geology and Geophysics, v. 6, p. 56–65 (in Russian).

Fedorenko, V.A., Lightfoot, P.C., Naldrett, A.J., Czamanske, G.K, Hawkesworth, C.J., Wooden, J.L., and Ebel, D.S., 1996, Petrogenesis of the flood-basalt sequence at Noril'sk, north central Siberia: International Geology Review, v. 38, p. 99–135.

Genkin, A.D., Distler, V.V., Gladyshev, G.D., Filimonova, A.A., Yevstigneeva, T.L., Kovalenker, V.A., Laputina, I.P., Smirnov, A.V., and Grokhovskaya, T.L., 1981, Sulfide copper-nickel ores of the Noril'sk deposits: Moscow, Nauka, 234 p. (in Russian).

Ghiorso, M.S., and Sack, R.O., 1995, Chemical mass transfer in magmatic processes. IV. A revised and internally consistent thermodynamic model for the interpolation and extrapolation of liquid-solid equilibria in magmatic systems at elevated temperatures and pressures: Contributions to Mineralogy and Petrology, v. 119, p. 197–212.

Gorbachev, N.S., and Grinenko, L.N., 1973, The sulfur-isotope ratios of the sulfides and sulfates of the Oktyabr'sky sulfide deposit, Noril'sk region, and the problem of its origin: Geokhimiya, v. 8, p. 1127–1136.

Grinenko, L.N., 1985, Sources of sulfur of the nickeliferous and barren gabbro-dolerite intrusions of the northwest Siberian platform: International Geology Review, v. 28, p. 695–708.

Hawkesworth, C.J., Lightfoot, P.C., Blake, S., Naldrett, A.J., Doherty, W., Fedorenko, V.A., and Gorbachev, N.S., 1995, Magma differentiation and mineralisation in the Siberian continental flood basalts: Lithos, v. 34, p. 61–68.

Horan, M.F., Walker, R.J., Fedorenko, V.A., and Czamanske, G.K., 1995, Os and Nd isotopic constraints on the temporal and spatial evolution of flood basalt sources, Siberia: Geochimica et Cosmochimica Acta, v. 59, p. 5159–5168.

Janecky, D.R., and Shanks, W.C., III, 1988, Computational modeling of chemical and sulfur isotopic reaction processes in seafloor hydrothermal systems: Chimneys, massive sulfides, and subjacent alteration zones: Canadian Mineralogist, v. 26, p. 805–825.

Kamo, S.L., Czamanske, G.K., and Krogh, T.E., 1996, A minimum U-Pb age for Siberian flood-basalt volcanism: Geochimica et Cosmochimica Acta, v. 60, p. 3505–3511.

Kamo, S. L., Czamanske, G.K., Amelin, Y., Fedorenko, V.A., and Trofimov, V.R., 2000, U-Pb zircon and baddeleyite, and U-Th-Pb perovskite ages for Siberian flood volcanism, Maymecha-Kotuy area, Siberia [abs.]: Goldschmidt Conference 2000, Oxford, England, September 3–8, Journal of Conference Abstracts, p. 569.

Latypov, R.M., 2002, Phase equilibria constraints on relations of ore-bearing intrusions with flood basalts in the Noril'sk region, Russia: Contributions to Mineralogy and Petrology, v. 143, p. 438–449.

Leeman, W.P., and Lindstrom, D.J., 1978, Partitioning of Ni^{2+} between basaltic and synthetic melts and olivines: An experimental study: Geochimica et Cosmochimica Acta, v. 42, p. 801–806.

Li, C., and Ripley, E.M., 2002, The effect of Ni-S speciation on nickel partitioning in olivine [abs.]: Geochimica et Cosmochimica Acta, v. 66, p. A452.

Li, C., Lightfoot, P.C., Amelin, Y.V., and Naldrett, A.J., 2000, Contrasting petrological and geochemical relationships in the Voisey's Bay and Mushuau intrusions, Labrador, Canada: Implications for ore genesis: Economic Geology, v. 95, p. 771–799.

Li, C., Maier, W.D., and de Waal, S.A., 2001, The role of magma mixing in the genesis of PGE mineralization of the Bushveld Complex: Thermodynamic calculation and new interpretations: Economic Geology, v. 96, p. 653–662.

Li, C., Ripley, E.M., Maier, W.D., and Gomwe, T.E.S, 2002, Olivine and sulfur isotopic compositions of the Uitkomst Ni-Cu sulfide ore-bearing complex, South Africa: Evidence for sulfur contamination and multiple magma emplacements: Chemical Geology, v. 188, p. 149–159.

Lightfoot, P.C., and Hawkesworth, C.J., 1997, Flood basalts and magmatic Ni, Cu, and PGE sulfide mineralization: Comparative geochemistry of the Noril'sk (Siberian traps) and West Greenland sequences: American Geophysical Union Monograph, v. 100, p. 357–380.

Lightfoot, P.C., Naldrett, A.J., Gorbachev, N.S., Doherty, W., and Fedorenko, V.A., 1990, Geochemistry of the Siberian trap of the Noril'sk area, USSR, with implications for the relative contributions of crust and mantle to flood basalt magmatism: Contributions to Mineralogy and Petrology, v. 104, p. 631–644.

Lightfoot, P.C., Hawkesworth, C.J., Hergt, J., Naldrett, A.J., Gorbachev, N.S., Fedorenko, V.A., and Doherty, W., 1993, Remobilisation of continental lithosphere by mantle plumes: Major, trace element, and Sr-, Nd-, and Pb-isotope evidence for picritic and tholeiitic lavas of the Noril'sk district, Siberian trap, Russia: Contributions to Mineralogy and Petrology, v. 114, p. 171–188.

Lightfoot, P.C., Naldrett, A.J., Gorbachev, N.S., Fedorenko, V.A., Hawkesworth, C.J., and Doherty, W., 1994, Chemostratigraphy of Siberian trap lavas, Noril'sk district, Russia: Implications and source of flood basalt magmas and their associated Ni-Cu mineralization: Ontario Geological Survey Special Publication 5, p. 283–312.

Likhachev, A.P., 1994, Ore-bearing intrusions of the Noril'sk region: Ontario Geological Survey Special Publication 5, p. 185–202.

Moore, J.G., 1970, Water content of basalt erupted on the ocean floor: Contributions to Mineralogy and Petrology, v. 28, p. 272–279.

Naldrett, A.J., and Lightfoot, P.C., 1993, Ni-Cu-PGE ores of the Noril'sk region, Siberia: A model for giant magmatic sulfide deposits associated with flood basalts: Society of Economic Geologists Special Publication 2, p. 81–123.

——1999, Ni-Cu-PGE deposits of the Noril'sk region, Siberia: Their formation in conduits for flood basalt volcanism: Geological Association of Canada Short Course Notes, v. 13, p. 195–250.

Naldrett, A.J., Lightfoot, P.C., Fedorenko, V., Doherty, W., and Gorbachev, N.S., 1992, Geology and geochemistry of intrusions and flood basalts of the Noril'sk region, USSR, with implications for the origin of the Ni-Cu ores: Economic Geology, v. 87, p. 975–1004.

Naldrett, A.J., Fedorenko, V.A., Lightfoot, P.C., Kunilov, V.E., Gorbachev, N.S., Doherty, W. and Johan, Z., 1995, Ni-Cu-PGE deposits of the Noril'sk region, Siberia: Their formation in conduits for flood basalt volcanism: Transactions of the Institute of Mining and Metallurgy, v. 104, p. B18–B36.

Naldrett, A.J., Fedorenko, V.A., Asif, M., Lin, S., Kunilov, V.A, Stekhin, A.I., Lightfoot, P.C., and Gorbachev, N.S., 1996, Controls on the compositions of Ni-Cu sulfide deposits as illustrated by those at Noril'sk, Siberia: Economic Geology, v. 91, p. 751–773.

Ripley, E.M., Lightfoot, P.C., Li, C., and Elswick, E.R., in press, Sulfur isotopic studies of continental flood basalts in the Noril'sk region: Implications for the association between lavas and ore-bearing intrusions: Geochimica et Cosmochimica Acta.

Roeder, P.L., and Emslie, R.F., 1970, Olivine-liquid equilibrium: Contributions to Mineralogy and Petrology, v. 71, p. 257–269.

Snyder, D.A. and Carmichael, I.S.E., 1992, Olivine-liquid equilibria and chemical activities of FeO, NiO, Fe_2O_3, and MgO in natural basic melts: Geochimica et Cosmochimica Acta, v. 56, p. 303–318.

Walker, R.J., Morgan, J.W., Horan, M.F., Czamanske, G.K., Krogstad, E.J., Likhachev, A.P., and Kunilov, V.E., 1994, Re-Os isotopic evidence for an enriched-mantle plume source for the Noril'sk-type ore-bearing intrusions, Siberia: Geochimica et Cosmochimica Acta, v. 58, p. 4179–4197.

Wooden, J.L., Czamanske, G.K., Bouse, R.M, Likhachev, A.P., Kunilov, V.E., and Lyul'ko, V., 1992, Pb isotope data indicate a complex mantle origin for the Noril'sk-Talnakh ores, Siberia: Economic Geology, v. 87, p. 1153–1165.

Wooden, J.L., Czamanske, G.K., Fedorenko, V.A., Arndt, N.T., Chauvel, C., Bouse, R.M., King, B-S.W., Knight, R.J., and Siems, D.F., 1993, Isotopic and trace element constraints on mantle and crustal contributions to characterization of Siberian continental flood basalts, Noril'sk area, Siberia: Geochimica et Cosmochimica Acta, v. 57, p. 3677–3704.

Zen'ko, T.E., and Czamanske, G.K., 1994a, Physical and petrologic aspects of the intrusions of the Noril'sk-Talnakh ore junctions, Siberia: Ontario Geological Survey Special Publication 5, p. 263–282.

——1994b, Tectonic controls on ore-bearing intrusions of the Talnakh ore junction: Position, morphology, and ore distribution: International Geology Review, v. 36, p. 1033–1057.

Zientek, M.L., Likhachev, A.P., Kunilov, V.I., Barnes, A.-J., Meier, A.L., Carlson, R.R., Briggs, P.H., Fries, T.L., and Adrian, B.M., 1994, Cumulus processes and the composition of magmatic ore deposits: Examples from the Talnakh district, Russia: Ontario Geological Survey Special Publication 5, p. 373–392.